

BEHAVIORAL AND NEURAL MECHANISMS UNDERLYING SPATIAL
EXPLORATION AND DECISION

A DISSERTATION
SUBMITTED TO THE FACULTY OF THE GRADUATE SCHOOL
OF THE UNIVERSITY OF MINNESOTA
BY

Sofia Sakellaridi

IN PARTIAL FULFILLMENT OF THE REQUIREMENTS
FOR THE DEGREE OF
DOCTOR OF PHILOSOPHY

Apostolos P. Georgopoulos & Matthew V. Chafee , Co-Advisors

JUNE 2014

Acknowledgements

I would like to express my deep gratitude to my advisers Professor Apostolos P. Georgopoulos and Professor Matthew V. Chafee, who have been tremendous mentors for me over the years. Their guidance, unfailing support, and enthusiastic encouragement allowed me to grow as a research scientist and as a person. I would also like to thank Professor Art Leuthold and Professor Victoria Interrante for their willingness to serve as my committee members and for their brilliant comments and suggestions. I would like to extend my thanks to Professor Art Leuthold for his assistance with the MEG study, and Peka Christova for her suggestions and assistance with the collection of the data.

My very great appreciation to my officemates at the Brain Sciences Center for all the cooperation. I owe a lot to my friends in Greece and the US, who were very supportive and made my life happier during the often tough times of my PhD pursuit.

A special thanks to my family. Words cannot express how grateful I am to my parents, my sister, and my grandparents for all the love and the support they provided me through my entire life. They were there for me in so many ways, even though they live so far away.

Last but not least, I would like to thank my partner Vassilis, for his love, patience, and encouragement. He was always my support and stood by me through the good times and bad.

Dedication

This dissertation is dedicated to my dad, who was a source of inspiration to me throughout my life, and made me who I am today.

Abstract

The ability to explore novel environments and make decisions is a fundamental component of human and animal behavior. Even though significant progress has been made in recent years in understanding the mechanisms of exploration and decision-making, little is known on how the brain extracts, encodes and processes information from the environment to make decisions.

The primary goal of this thesis is to understand the behavioral and neural mechanisms underlying the processing of spatial information, acquired during exploration of realistic environments to make spatial decisions. We designed a novel task, in which subjects had to explore maps from various U.S. cities to decide where to build a City Hall, while neuromagnetic fluxes were recorded from their heads using a whole-head MEG device. We found that ongoing neuronal activity in a network of cortical regions was associated with particular spatial parameters of the city maps. This network involved predominantly the right frontal and prefrontal areas of the brain, suggesting that these areas have an important role in processing spatial information for making decisions. Additionally, we found other brain areas that were also involved in the processing of spatial information, such as right temporal areas and the cerebellum. These results indicate that processing spatial information for making a decision is a complex process that requires the involvement of more than one regions. Finally, we found that the associations between changes in the ongoing neural activity and

spatial parameters were modulated by the street network type. This suggests that, depending on the type of street network, people may use different spatial information to explore the map and make a spatial decision.

We also studied how people make spatial decisions in realistic environments when they were forced to select between a limited set of choices. In this experiment, individuals had to explore maps from various U.S. cities, but now to select between two locations to build a hypothetical Post Office. We recorded subjects' eye positions and analyzed the gaze behavior to characterize how people explored maps to select between these options. We found that subjects were continuously exploring the areas around the two options and the center of the map, by looking back and forth between them before making a decision. Unlike economic choices, in which people follow similar strategies by looking repeatedly at the available options, in our experiment individuals were also exploring the area around the center of the map. These findings suggest that the subjects might have mentally placed themselves at the center of the map and evaluated the alternative options with respect to their current location. We also found other similarities with economic choice paradigms, such as people spent more time exploring the area around the option ultimately chosen. Finally, subjects showed a strong bias to select the option they initially explored.

Contents

List of Tables	viii
List of Figures	ix
1 Introduction	1
1.1 Exploring and navigating in real environments	1
1.2 Neural mechanisms of exploration and navigation in animals	3
1.3 Neural substrates of spatial exploration and navigation in humans . .	4
1.3.1 Neurophysiological and clinical studies in patients	4
1.3.2 Modern neuroimaging techniques reveal complex brain networks in exploration and navigation	7
1.4 Making spatial decisions in real environments	14
1.4.1 Decision making and gaze behavior	15
1.4.2 Neural mechanisms of decision making	19
1.5 Exploring small city maps to make spatial decisions	24
1.5.1 Spatial characteristics of city maps	25
1.5.2 Neural mechanisms underlying exploration of city maps and choice of destination	27
1.5.3 Behavioral mechanisms underlying spatial decisions with instructed- choices	29

2	Neural mechanisms underlying the exploration of small city maps using magnetoencephalography	31
2.1	Overview	31
2.2	Introduction	33
2.3	Materials and methods	37
2.3.1	Participants	37
2.3.2	Stimuli	37
2.3.3	Experimental Paradigm	38
2.3.4	Data acquisition	40
2.3.5	Data preprocessing	43
2.3.6	Time series analysis	43
2.3.7	Map Parameters	44
2.3.8	Analysis of the relations between neural activity and map parameters	47
2.4	Results	51
2.4.1	Prewhitening neural data	51
2.4.2	Map parameters	53
2.4.3	Relation between neural activity and map parameters	61
2.5	Discussion	66
3	Cognitive mechanisms underlying instructed choice exploration of small city maps	73
3.1	Overview	73
3.2	Introduction	74
3.3	Materials and methods	77
3.3.1	Subjects	77

3.3.2	Stimuli	78
3.3.3	Experimental Paradigm	80
3.4	Results	84
3.4.1	Decision Time	84
3.4.2	Spatial characteristics of eye positions	85
3.4.3	Time spending in exploring the alternative options and choice biases	88
3.4.4	Comparison of alternative options as a function of time	89
3.5	Discussion	93
4	Concluding Remarks	98
4.1	Summary	98
4.2	Broader impacts	100
	Bibliography	102

List of Tables

2.1	Number of cases, mean, and standard deviation of space syntax parameters across <i>regular grids</i> for each subject.	58
2.2	Number of cases, mean, and standard deviation of space syntax parameters across <i>colliding grids</i> for each subject.	58
2.3	Number of cases, mean, and standard deviation of space syntax parameters across <i>curvilinear grids</i> for each subject.	59
2.4	Number of cases, mean, and standard deviation of space syntax parameters across <i>cul-de-sacs</i> for each subject.	59
2.5	Number of cases, mean, and standard deviation of space syntax parameters across <i>supergrids</i> for each subject.	60

List of Figures

2.1	Map stimuli. Each row corresponds to stimuli of the same street network type. There are totally 20 stimuli, 4 stimuli per street network type.	39
2.2	Task sequence. (A) Trial starts with the presentation of an open circle on the center of a black screen. (B) The subject is required to fixate eyes and place the mouse inside the circle for 1.5 s. (C) The stimulus is presented and subject explores the map by moving his/her eyes in order to decide where to place a hypothetical City Hall. (D) The subject chooses the City Hall location by clicking the mouse at the desired position.	40
2.3	(A) Subject lays supine in the recording chamber with head inside the cryogenic helmet-shaped dewar. (B) The 248-sensor whole-head MEG system is located inside a shielded room that reduces electromagnetic and environmental noise.	41
2.4	2D projection of the 248-channel axial gradiometer MEG system used to record brain activity.	42

2.5	Parts of the map defined by the circular areas of 6 degrees of visual angle radius centered on instantaneous x - y eye positions were analyzed by space syntax characteristics. The red dot marks an eye fixation on the map, and blue circle corresponds to the circular area of 6 DVA radius centered on this eye position.	45
2.6	Subject 2 MEG raw data (29.93 s for 20 trials) from sensor 1 (A) before and (B) after applying ARIMA(25,1,1) modeling.	51
2.7	ACF structure of the MEG signal recorded from sensor 1 (subject 2) before (A) and after (B) applying an ARIMA(25,1,1) model. PACF structure of the MEG signals recorded from the same sensor before (C) and after (D) applying the model. The black lines that are close to the reference zero-line, denote 95% statistical significance level from the ACF and PACF value. Notice that the strong autocorrelation and partial-autocorrelation structure on the raw data disappeared after applying ARIMA(25,1,1) modeling. That is, the ACFs and PACFs are flat.	52
2.8	ACF structure of number of street intersections from subject 2 before (A) and after (B) applying an ARIMA(25,1,1) model. PACF structure of number of street intersections recorded from the same subject before (C) and after (D) applying the model. The black lines that are close to the reference zero-line, denote 95% statistical significance level from the ACF and PACF value. Notice that the strong autocorrelation and partial-autocorrelation structure on the raw data disappeared after applying ARIMA(25,1,1) modeling. That is, the ACFs and PACFs are flat.	54

2.9	ACF structure of total street length from subject 2 before (A) and after (B) applying an ARIMA(25,1,1) model. PACF structure of total street length recorded from the same subject before (C) and after (D) applying the model. The black lines that are close to the reference zero-line, denote 95% statistical significance level from the ACF and PACF value. Notice that the strong autocorrelation and partial-autocorrelation structure on the raw data disappeared after applying ARIMA(25,1,1) modeling. That is, the ACFs and PACFs are flat. . .	55
2.10	ACF structure of regularity index from subject 2 before (A) and after (B) applying an ARIMA(25,1,1) model. PACF structure of regularity index recorded from the same subject before (C) and after (D) applying the model. The black lines that are close to the reference zero-line, denote 95% statistical significance level from the ACF and PACF value. Notice that the strong autocorrelation and partial-autocorrelation structure on the raw data disappeared after applying ARIMA(25,1,1) modeling. That is, the ACFs and PACFs are flat. . .	56
2.11	Mean \pm standard error of mean of (A) number of street intersections, (B) total street length, and (C) regularity index, across 10 subjects for each street network type.	57
2.12	Spatial distributions of the neural processing of (A) number of street intersections, (B) total street length, and (C) regularity index, across all street network types. 2-D contour plots in the MEG sensor space of the mean absolute t -values ($P < 0.05$) across 10 subjects corresponding to the regression coefficients of space syntax parameters in the linear regressions, Eq. (2.4)-(2.6).	62

2.13	Spatial distributions of the neural processing of <i>number of street intersections</i> for each street network type. First row illustrates example stimuli from (A) regular, (B) colliding, (C) curvilinear, (D) cul-de-sac, and (E) supergrid street network layouts. Second row illustrates 2-D contour plots in the MEG sensor space of the mean absolute t -values across 10 subjects ($P < 0.05$) corresponding to the regression coefficients of number of street intersections in the linear regressions for each street network type respectively, Eq. (2.4).	63
2.14	Spatial distributions of the neural processing of <i>total street length</i> for each street network type. First row illustrates example stimuli from (A) regular, (B) colliding, (C) curvilinear, (D) cul-de-sac, and (E) supergrid street network layouts. Second row illustrates 2-D contour plots in the MEG sensor space of the mean absolute t -values across 10 subjects ($P < 0.05$) corresponding to the regression coefficients of total street length in the linear regressions for each street network type respectively, Eq. (2.5).	64
2.15	Spatial distributions of the neural processing of <i>regularity index</i> for each street network type. First row illustrates example stimuli from (A) regular, (B) colliding, (C) curvilinear, (D) cul-de-sac, and (E) supergrid street network layouts. Second row illustrates 2-D contour plots in the MEG sensor space of the mean absolute t -values across 10 subjects ($P < 0.05$) corresponding to the regression coefficients of regularity index in the linear regressions for each street network type respectively, Eq. (2.6).	65

2.16	Dendrogram (using the average linkage between groups) displaying the clusters resulting by joining the grids that are most similar, in terms of their spatial distributions in the MEG sensor space of the absolute t -values corresponding to the number of street intersections.	67
2.17	Dendrogram (using the average linkage between groups) displaying the clusters resulting by joining the grids that are most similar, in terms of their spatial distributions in the MEG sensor space of the absolute t -values corresponding to the number of total street length.	67
2.18	Dendrogram (using the average linkage between groups) displaying the clusters resulting by joining the grids that are most similar, in terms of their spatial distributions in the MEG sensor space of the t -absolute values corresponding to the regularity index.	68
3.1	Map stimuli. Magenta dots denote the two potential locations (targets) for the Post Office. Blue dot marks the center of the map (shown here for illustration purposes).	79
3.2	Task sequence. (A) Trial starts with the presentation of an open circle on the center of a black screen. (B) The subject is required to fixate eyes and place the mouse inside the circle for 1.5 s. (C) The stimulus is presented and subject explores the map by moving his/her eyes in order to decide between two alternative positions to place a hypothetical Post Office. (D) Subject chooses the Post Office location by clicking the mouse at the desired position.	80

3.3	A single trial illustrating the eye positions (black and red dots) of a subject. Magenta dots mark the two targets, blue dot denotes the center of the map, and green diamond marks the selected target. Blue circles correspond to the circular areas of 2, 4, 6 and 8 degrees of visual angle radius centered on the two targets and the center of the map, and red dots are the eye positions within the areas of 4 DVA radius.	83
3.4	Superimposed eye positions (black dots) on each map of all 12 subjects, and the corresponding isolines illustrating the probability density of the eye positions. Isoline colors describe different levels (0 to 1) of the contour intervals, with red corresponding to high probability density values, and blue corresponding to low density values.	86
3.5	Average density (mean \pm SEM, $N = 236$ trials) of eye positions for selected targets (red), non-selected targets (blue), center of the map (magenta), and the combination of them (white) , calculated in the circular areas of 2, 4, 6, and 8 degrees of visual angle radius centered on each one of them.	87
3.6	Average relative density of eye positions for selected and non-selected targets in the circular areas of 4 degrees of visual angle centered on each target (mean \pm SEM, $N = 209$ trials).	89
3.7	Example trials of single subjects while exploring different types of maps - one for each street network type - illustrating the <i>logarithmic ratio distance</i> (Eq. 3.1) of instantaneous eye positions to selected target over the non-selected target. Negative values of the log-ratio distance correspond to eye positions closer to the target ultimately selected, and vice-versa.	91

3.8	Mean logarithmic ratio (mean \pm SEM, $N = 236$ trials) of the Euclidean distance of the ongoing eye position to the selected target to the Euclidean distance of the eye position to the non-selected target, for 1 s after stimulus presentation. Trials are aligned to stimulus presentation. Notice that as early as 230 ms after stimulus onset, values of the mean log-ratio distance become negative (i.e., eyes are closer to the target ultimately selected).	92
3.9	Mean logarithmic ratio (mean \pm SEM, $N = 236$ trials) of the Euclidean distance between the ongoing eye position and the selected target, to the distance between the eye position and the non-selected target, for 1 s before target selection. Trials are aligned to target selection. 345 ms before the selection of the target, mean log-ratio distance values become negative (i.e., subjects on average placed their eyes closer to the target ultimately selected).	93
3.10	Mean Logarithmic Ratio Distance vs. SEM for the 345 ms before the selection of the target (see Fig.3.9). Red line describes the quadratic fit ($r^2=0.730$, $P=0.0001$) of this relation.	94

Chapter 1

Introduction

1.1 Exploring and navigating in real environments

On a daily basis, the physical world poses a number of problems to solve. For most of these problems, humans and animals have to explore and navigate within the environment and make spatial decisions. For instance, animals continuously explore their surroundings to localize food, avoid predators, and find places to live. On the other hand, people have to solve more sophisticated spatial decision problems. When traveling or visiting a city for the first time, we are usually interested in finding points of interests, such as museums, theaters, and other attractions. Before even booking a hotel or deciding at which restaurant we will have lunch on Sunday with family, we might like to locate the place and explore its surroundings to find out if there are fun activities nearby. When selecting a locale to live, we are taking into account the realities of spatial organization. Solving all these problems requires

cognitive capabilities to extract information from the environment and combine it with other factors (e.g., prior knowledge) to make a decision. Such cognitive skills involve spatial exploration, memory, and navigation. To appreciate the importance of these remarkable abilities, recall the times that you have gotten lost, maybe in a new city, heading in the wrong direction or walking in circles on the way to your hotel.

The question of how people and animals explore and navigate within the environment has been a topic of many research studies since the pioneering work of Edward Tolman and the concept of cognitive maps [79]. Tolman noted a quite interesting behavior reported by Lashley in 1929, when one of his rats, after having learned a maze, escaped accidentally near the starting box and ran directly to the goal-box where the food was located. This finding suggested that the rat had an internal allocentric (i.e., world-centered) representation of space, or a cognitive map of its environment. To test the cognitive map hypothesis, Tolman conducted a series of experiments in which he trained rats in an alley maze that offered food at the end. Then, rats were moved into a sunburst pattern maze consisting of alleys radiating at about 15-degree intervals, and the straight-ahead alley, which corresponded to the trained path, was blocked. Tolman noticed that the most popular alternative path that rats took was the alley that pointed almost directly to the place where the food had previously been located. Based on this finding, he suggested that rats had internalized the makeup of the maze in their brains, which allowed them to take novel paths when the learned path was blocked.

1.2 Neural mechanisms of exploration and navigation in animals

Since the pioneering work of Tolman, a series of studies have contributed to the understanding of the behavioral and neural mechanisms of spatial cognition. One of the most important breakthroughs was the discovery of place cells, which are pyramidal cells in the rat hippocampus that exhibit high firing rate when the animal is located in a specific location within its environment corresponding to the cell’s “place field” [45]. As different place cells have different place fields and since damage to the hippocampus may result in disrupted spatial orientation, it was proposed that hippocampus is the key neural structure of these mental maps of space [46].

Most recently, head direction cells were discovered in the postsubiculum coding for rat’s orientation [77], and grid cells were found in the medial entorhinal cortex firing when the rat is at specific locations in its surroundings (a grid cell’s so called firing fields). These grid fields form a regular hexagonal grid-like spacing across the rat’s environment [25]. Other studies have also explored the neural basis of allocentric spatial representation in the hippocampus and posterior parietal cortex of monkeys [64, 72].

Theta rhythm has been observed in rodents during spatial exploration and navigation and is thought to be involved in such tasks [47]. Specifically, hippocampal place cells systematically change their phase of firing relative to theta as the rat moves through a place field. This finding suggests that one function of theta is to provide a

reference frame for a neural code in which different spatial information is represented at different phases of the theta cycle.

Although these studies offer important insights into the neural structures underlying spatial cognition, there is a limit to what we can find out using experimental animals. Single-unit recordings on freely moving animals produce sensory-motor confounds, and, on the other hand, people explore and navigate within more complex environments, and solve more sophisticated spatial decision problems.

1.3 Neural substrates of spatial exploration and navigation in humans

1.3.1 Neurophysiological and clinical studies in patients

In humans, the experimental study of hippocampus and other brain areas that might be related to exploration, navigation, and spatial decisions is limited by practical and ethical reasons. The hippocampus is located in the medial temporal lobe, an area not easy to access, and researchers cannot operate on or damage a healthy human brain to try to unravel its functions.

However, a recent study reported the first single-unit recording investigation underlying human exploration and navigation, and provided evidence for homologues of place cells in humans [22]. Single neuronal responses were recorded from the hippocampus, amygdala, parahippocampal, and prefrontal cortices of seven patients with

pharmacologically intractable epilepsy, while they were playing the taxi driver in a computer game. Particularly, participants had to explore a small virtual reality town searching for passengers and take them to their destinations. Cells' firing rates were compared as a function of the subject's location in town ("place"), the object they could see ("view"), and where they were trying to get to ("goal"). Results showed that cells which responded to places were clustered mainly in the hippocampus and secondarily in parahippocampus, whereas cells which responded to views of landmarks were topographically organized mainly in the parahippocampus. This study offered unique insight into the mechanisms of human spatial exploration and navigation, and, together with the discovery of place cells in rats and non-human primates, it supports the idea that the human hippocampus is a key neural structure involved in the representation of allocentric space.

Clinical studies in patients with brain lesions have also contributed to the understanding of the neural basis of spatial cognition. In accord with the idea of cognitive maps and the discovery of place cells, the hippocampus seems to be involved in facilitating spatial memory in the form of exploration and navigation. Specifically, early studies of the amnesic patient H. M., who had sustained a bilateral medial temporal lobe resection, suggested that the hippocampus is associated with episodic memory (i.e., the memory for experienced events) [68]. Later studies have examined temporal lobe involvement in human topographical memory, i.e., the ability to orient oneself in space, to recognize and follow an itinerary, or to recognize familiar places. Particularly, Maguire and colleagues investigated the effects of unilateral temporal

lobectomy on topographical memory [41]. They showed both controls and patients with left or right temporal lobectomy a film footage of two overlapping walked routes through a town. Then, subjects' topographical memory of the town was tested by assessing their ability to judge proximity between groups of three landmarks presented as pictures, distances between pairs of landmarks, the correct sequence of landmarks along the walked routes, and their ability to draw accurate sketch maps of the town. Results suggested that both left and right temporal lobes are required for navigation and way-finding in the environment, although the left temporal lobectomy patient group was impaired on all topographical tasks (with the exception of the proximity judgment test) relative to the control group, but to a lesser degree than the right temporal lobectomy group. Spiers and colleagues extended this work by using the realistic and large-scale environment of a virtual reality town to study the effects of right or left anterior temporal lobectomy on topographical and episodic memory [31]. After exploring the town, topological memory was tested by requiring subjects to navigate to specific locations in the town, recognize previously visited locations, and draw maps of the town. Episodic memory was assessed by testing the retrieval of simulated events which consisted of collecting objects from characters while following a route through the virtual town. Results were consistent with the view that the hippocampus is involved in navigation, and suggested that the right medial temporal lobe is mostly involved in topographical memory, whereas the left medial temporal lobe mediates context-dependent aspects of episodic memory.

1.3.2 Modern neuroimaging techniques reveal complex brain networks in exploration and navigation

Despite the significant contribution of neurophysiological and clinical studies in elucidating the neural mechanisms underlying spatial cognition, they are limited by the fact that “they do not see the whole brain”. Recent advancements in non-invasive brain imaging techniques, such as functional Magnetic Resonance Imaging (fMRI), Positron Emission Tomography (PET), electroencephalography (EEG) and magnetoencephalography (MEG) enable us to study the brain networks underlying spatial exploration, and navigation.

fMRI and PET have high spatial resolution, but are limited in temporal resolution to approximately 3 to 20 s respectively, because they measure brain activity indirectly. fMRI uses a strong magnetic field to measure variations in the Blood Oxygenation Level Dependent (BOLD) signal over time as the neural activity changes in a given brain area, and PET measures the flow of blood to different areas of the brain. On the other hand, MEG and EEG measure the magnetic/electrical activity of the brain and are able to follow changes in neural synaptic activity on a millisecond time scale. In both MEG and EEG, sensors are arranged on the surface of the head, however, MEG sensors do not touch the head. MEG sensors record the synchronous synaptic activity of thousands of neurons in the brain regions near the sensors, whereas EEG sensors measure the associated scalp potentials.

Brain areas for exploration and navigation

Recent imaging studies have revealed a widespread network of brain structures that seem to be involved in spatial exploration and navigation. Hippocampus and parahippocampal gyrus, posterior cingulate cortex, parts of the basal ganglia, parietal lobe, and prefrontal cortex are some of the key brain regions for human spatial exploration and navigation.

Using fMRI, Aguirre and colleagues recorded the brain activity of healthy subjects while exploring and then navigating in a virtual reality maze [2]. Results showed increased activity in parahippocampal gyrus but not the hippocampus during both learning (exploration phase) and recall (navigation phase) of topographic information. These findings suggest that the parahippocampal gyrus might be the key structure that supports spatial mapping in humans. Furthermore, significant activity across subjects was observed in the right premotor area as well as bilaterally in the superior posterior parietal, posterior cingulate, lingual gyrus, posterior medial-temporal areas, and cerebellum. The authors suggested that since spatial information processing involves transformation of the coordinate frame in which stimuli are coded, the activity observed in parietal and posterior cingulated cortex is likely to reflect recruitment of this spatial processing. This view is also supported by other studies, according to which the posterior parietal cortex may be involved in translating egocentric (i.e., body centered) to allocentric information and vice versa [8]. Egocentric representations are thought to be based on neurons in the medial parietal area (precuneus) that

encode the distance and directions of environmental landmarks, whereas allocentric representations mainly involve the hippocampus and parahippocampus [8].

A later study attempted to characterize the brain network involved in human navigation and provided a more precise interpretation of the roles of each of these areas. Subjects were scanned using PET while they navigated a previously experienced virtual reality town [40]. Activation of right hippocampus was associated with participants' accuracy of navigation (accuracy was computed as the absolute difference between the subject's heading direction and the direction of the destination at each meter along the subject's trajectory), whereas activation of left hippocampus was correlated with success of navigation (successful trials were the ones in which the correct destination was reached). Bilateral medial and right inferior parietal cortex activity corresponded to movement through the environment, and prefrontal cortex was correlated with success in navigating around blocked routes. Finally, caudate activation was associated with subjects' speed of navigation. These findings imply that parietal cortex and hippocampus may cooperate to enable navigation to an unseen goal. Specifically, hippocampus may provide an allocentric spatial representation, allowing the computation of the direction from any start to any goal location, whereas right inferior parietal cortex may use this information to compute an egocentric representation, which is essential to compute body turns and movements towards the goal. These suggestions are also supported by neuroanatomical tracing studies, which showed strong projections between inferior parietal lobe and medial temporal structures, implying functional connectivity between those areas [76].

In a later study, Spiers and Maguire tried to explore neural activity corresponding to more detailed aspects of navigation. They used fMRI to measure brain activity of taxi drivers while they were operating a taxi in a computer game, in which they had to drive around central London in response to requests from customers [73]. At the end of the task, taxi drivers observed a playback of their trip, and answered questions about what they were thinking at various points during their trip. This helped experimenters to break down the task into many more subcomponents, such as visual inspection, action planning, coasting, and others. Results revealed a wide network of brain structures involved in the initial planning of the route, including the hippocampus, and lateral and medial prefrontal areas. When subjects changed their routes during navigation, right parietal, retrosplenial and prefrontal areas were activated. In concordance with a role in egocentric spatial processing [8,40], posterior parietal cortex was active when subjects were navigating. The observed dorsomedial prefrontal cortex was active mostly during route planning, which is compatible with the prevailing view that this area is involved in monitoring responses in situations of uncertainty and altering behavior to adapt to the environment [63]. Also, activation of the lateral prefrontal cortex whenever subjects encountered unexpected obstructions, such as a blocked route, is consistent with previous studies linking this area to detecting violations of expected previously learned associations [16].

Neural representation of objects relevant for navigation

So far all these studies provided new insights into understanding the specific roles of individual brain areas in spatial cognition. But how do people find their way through their environment? As we navigate through our environment, objects at navigationally relevant locations can serve as key landmarks. Behavioral studies have reported that objects placed at decision points (i.e., intersections) are more likely to be remembered later than objects placed at non-decision points [4].

Janzen and Turennout investigated the role of landmarks in navigation, by having people first watch a film sequence through a virtual museum, and then informing them that they were being trained to be guides in the museum, and their task was to remember the objects and the route [32]. Objects were located along the hallway of the museum and occurred either at an intersection (decision point objects) or at a simple turn (non-decision point objects). After the study phase, subjects performed a simple object recognition task while in an fMRI scanner. They were presented with objects that had been in the museum, as well as with novel objects. The results revealed significantly larger activity in parahippocampal gyrus for decision point objects as compared with the non-decision point objects, for both remembered and forgotten objects. These findings suggest that the brain distinguishes objects used as landmarks to guide navigation, and therefore, it responds not only to the object itself but also to how relevant the object is for navigation. The increased activity in parahippocampal gyrus, is compatible with previous studies linking the activation of

this area when recalling landmarks [22, 42].

Neural code for navigation guiding

Janzen and Turennout provided evidence that the human brain distinguishes objects that are used as landmarks to guide navigation [32]. However, it is not clear how the brain guides navigation to goals. Spiers and Maguire tried to shed light on this question, by providing evidence for a navigational guidance system in the human brain [74]. Specifically, neural activity of subjects was recorded using fMRI while navigating to goal destinations in a virtual city. Researchers computed subjects' proximities (i.e., shortest linear distance) and egocentric directions to goal destinations at every second along every route, and examined the neural basis of these measures. Results showed that activity in medial prefrontal and right subicular/entorhinal areas is directly linked to goal proximity, whereas activity in posterior parietal cortex is correlated with egocentric direction to goals.

Although this work suggested that measures like goal proximity and egocentric direction to the goal are coded into the brain to guide navigation, it does not provide evidence for how brain makes decisions during navigation. Moreover, more direct measures of neural activity, such as MEG and EEG, would have been more appropriate to uncover more accurately the time course of the activity.

Theta oscillations and spatial exploration and navigation

Although fMRI is capable of achieving high spatial resolution, it is limited in temporal resolution to a time scale on the order of a few seconds. Given the importance of theta oscillations in rodents [47], it has been of interest to determine whether similar oscillations occur in humans. Hence, more direct measures of neural activity, such as EEG and MEG that sample at high rates to achieve temporal resolution on the order of milliseconds, have been utilized to study the association between navigation and oscillations in the theta frequency band (4-12 Hz). Theta oscillations were observed in a study in which epileptic patients were navigating in unfamiliar virtual reality mazes using intracranial EEG (iEEG), a method that uses electrodes to record EEG activity directly from the cortical surface [34]. These oscillations occurred in intermittent bouts and were present in widely separated cortical regions, including temporal and parietal cortex. The probability of their occurrence was related to task difficulty. However, it was unclear whether the increase in theta was due to the fact that participants were epileptic patients.

A more recent study used MEG to explore the spatiotemporal patterns of theta oscillations evoked when normal subjects performed various spatial tasks in a virtual reality city [20]. After exploring the virtual city (phase 1), subjects started navigating from a starting point to a destination until an obstruction was encountered at one of several possible locations along the main route (phase 2). At the appearance of the obstruction navigation was interrupted, and subjects had to contemplate a detour

(phase 3) and resume navigation until the destination was reached (phase 4). Results showed increased activity of signals in theta band that was stronger during navigation (phases 2 and 4) than during periods when subjects were not navigating (phases 1 and 3). Patterns of activity were mainly found bilaterally over temporal regions, and secondarily over frontal and parietal regions. Based on previous studies according to which medial temporal structures are involved in the formation of allocentric representation of space whereas parietal areas are associated with egocentric representation formation [40, 76], these findings suggest that the decrease in theta observed when subjects were retrieving a map from memory without navigating (phase 3) may be presumably due to non-participation of inferior parietal cortex.

1.4 Making spatial decisions in real environments

So far I have focused on reviewing studies about the mechanisms of exploration and navigation, neglecting an important component of human and animal behavior that is involved frequently during both exploration and navigation; spatial-decision making. Unless you are walking your leashed dog in a park or exploring a map of a city while you are drinking coffee, you almost always explore an environment to make a decision. For instance, animals explore their surroundings to localize food, avoid predators and find mates. Similarly, when visiting a city for the first time, you may explore it to find places for food, entertainment, etc. Hence, the main characteristic of this behavior is that exploration and navigation are goal-driven, which means that you explore and

navigate the environment to extract information and make a decision.

1.4.1 Decision making and gaze behavior

People and animals explore their surroundings by moving their eyes to extract information and identify potential actions. The relation between decision making and gaze behavior has been extensively documented in a series of human and animal studies but mostly in non-spatial contexts. For instance, a recent study showed that when people were asked to choose the most attractive between two given faces, their gaze was initially distributed evenly between them, but then was gradually biased towards the face eventually selected [69]. Another study argued against this finding claiming that gaze bias effects do not necessarily reflect preference choices, but constitute a more general characteristic of decision making [24]. In this study, individuals participated in a psychophysical experiment in which they were presented with photographic art images and asked to select the one they liked more (preference task), or the one they believed that was taken most recently (recency task). Interestingly, results showed that subjects had a strong bias toward the chosen item with respect to gaze duration, gaze frequency or both. This gaze effect was not task-dependent as the one reported previously on the experiment with the “attractive” faces [69], suggesting that gaze bias is likely a characteristic of decision making to extract information from the environment.

A recent study aimed to contribute on the debate on whether gaze effect is due

to “liking effect” (i.e., we fixate more on things we like) or due to information encoding aspects of decision-making process [67]. To address this question, researchers conducted a visual decision-making task similar to the one with the photographs discussed above [24], but now they used four different decision prompts: “Like”, “Dislike”, “Older” and “Newer”. Interestingly, results showed that gaze bias was present in all conditions except the “dislike” one, presumably because subjects’ preference to look at the item they liked when the goal was to identify the item they disliked compete. For the task that subjects had to decide whether a picture was new or old, results showed that gaze bias was modulated by the color of the picture, since color is a relevant feature for such decisions. Overall, these findings provide evidence that gaze bias was not modulated only by the “liking” effect, but also by any context-dependent decision variable.

A series of recent studies aimed to explore the relation between gaze behavior and decision making in economic choices. In these kinds of tasks, individuals have to select between alternative options that each one of them has a subjective value. Recent findings from neurophysiological studies suggest that decision variables associated with an option are integrated into a subjective value in prefrontal cortex [49,52]. This value is computed independently for each option and characterizes the “attractiveness” of this option with respect to the alternatives. The decision is made by comparing the subjective values of the alternative options, i.e., the option with the highest value is chosen. One important question that neuroscientists and economists aim to address is how people integrate information and compare values to select the

best option. Rangel and colleagues have conducted a series of psychophysical, computational modeling, and eye-tracking studies to explore the properties of the comparison process in economic choices [35, 36]. They found that when people are faced with multiple options in economic choice problems, they look repeatedly at them, presumably implementing a comparison process between the values of the options. This gaze behavior is consistent with real-world scenarios, such as when buying goods in a grocery store. Particularly, when selecting between two goods (e.g., a Fanta and a Coca-Cola) we look continuously back and forth between options and then make a choice, even if we have seen them before. So, why do people adopt this gaze behavior when choosing between items? Rangel and his colleagues suggested that eye fixations actually drive the comparison process. Using the eye positions recorded during economic choice tasks, and extending the popular drift-diffusion model (DDM), they showed that the subjective value of an item is biased by the time fixating that item. Hence, they suggested that looking repeatedly back and forth between the available options and fixating on them for a period of time is a decision-making process for integrating information and comparing the values of the options to make the best choice.

Even though all these studies provide important knowledge about gaze behavior in decision making, they are limited only to non-spatial context decisions. Gaze behavior both in humans and monkeys has been studied in way-finding tasks, i.e., find your way to navigate from a current location to a goal [9, 17]. In one of these studies, people had to view and mentally solve complex mazes by following a path through each maze

to find the end-point of the path [17]. There were 4 to 6 openings at the perimeter of each maze, four of which were labeled. One of these points was the entry point and the rest were potential exits marked by numbers. Subjects had to start from the entry point and press a computer key corresponding to the number of the true exit. In some trials, the path did not exit and subjects had to respond by typing zero. Analysis of gaze behavior revealed important findings on how people explored and solved these mazes. In particular, reaction time was positively correlated (i.e., increased) with the length of the main path, the number of turns, the direct distance from the entry to the end-point, and the presence of an exit. Additionally, the number of fixations increased as a function of the path length and the number of turns. Regarding the spatial characteristics of fixations, results showed that the eyes tended to fixate on main path (i.e., the path from the entrance to the exit) and follow it along its main course, such that fixations occurring later in time were positioned at progressively longer distance from the entrance. Importantly, the time people spent fixating at each point increased linearly with the length and the number of turns (i.e., length and complexity of the maze) in the path segment between the current point and the next fixation points. These results provide evidence that people processed the maze segment from the current fixation point to the next during the fixation time, and that a significant aspect of this spatial information processing involved the length and turns in that segment.

A recent study involves both way-finding and spatial decision making [83]. Participants were presented with screenshots of choice points selected from a large virtual

environment. Each screenshot showed an alternative path option. In one experiment, participants were free to choose between alternative path options to find an item hidden somewhere in the environment. In a second experiment, they were instructed to take a particular path as if following a guided route. Then, they were presented with screenshot images in random order and had to identify which path option they chose during initial exposure. Interestingly, in both experiments results showed a robust gaze bias towards the path that was eventually selected. Also, people spent more time fixating on areas where the local geometry of the environment changed (e.g., corners, openings, and occlusions). Researchers compared these experiments with two control experiments and concluded that gaze behavior and fixation patterns were specific to the spatial task. Therefore gaze bias effect is a general phenomenon in both non-spatial and spatial context decisions.

1.4.2 Neural mechanisms of decision making

After many years of intense research in neuroscience, it is still debatable how the brain evaluates the alternative options to make a decision. A classical theory in psychology and economics suggests that computation and comparison of values takes place within frontal areas, including mainly orbitofrontal cortex (OFC) and ventromedial prefrontal cortex (vmPFC) [44, 48, 50, 51]. The main characteristic of this “goods-based” theory is that decision making is a separate process from perception and action. Hence, when an individual is faced with multiple goods, different popu-

lations of neurons within frontal cortical areas represent the identities and the values of these goods. This representation is abstract in the sense that neurons encode the value of these goods irrespective of the sensorimotor contingencies (i.e., action costs required to get these goods) [50]. Therefore, the choice takes place within the “goods-space”, i.e., available goods are compared based on their values and the best option is selected.

The involvement of frontal regions in decision making was firstly reported in the famous “Phineas Gage” accident [19]. Phineas Gage (1848) was an American railroad construction foreman, whose frontal lobes were damaged when a iron rod was driven through his head. Even though this accident did not impair his memory, speech and motor skills, his personality changed dramatically. He became irritable, quick-tempered and could not make rational decisions [19]. Phineas Gage is not the only case that showed that high cognitive functions, such as decision-making and social cognition, are largely dependent upon the frontal areas of the brain. The next few years, series of clinical studies in patients with lesions localized in frontal lobes reported similar symptoms with Phineas Gage, i.e., impairment in the ability to predict the consequences of actions within complex environments [19]. Additionally, recent neurophysiological studies in non-human primates suggest the involvement of frontal areas, such as OFC, in the encoding of values of chosen options. Padoa-Schioppa with his colleagues conducted a series of single-unit recordings studies in monkeys during economic choices tasks [51]. Animals were presented with two types of juice, A and B, offered in different amounts, and were free to choose between them. Recording

activity from neurons in OFC showed that these neurons encode the value of the two goods irrespective of whether A is presented on the right and B on the left or vice-versa. Researchers claimed that these results indicate that the selection between alternative options is essentially a choice between goods rather than choice between actions.

All these studies provided apparent support to the “goods-based” theory. Even though this theory is efficient to explain a large variety of everyday decisions, such as selecting a restaurant to have dinner tonight or choosing where to invest our money, it is limited by the serial-order assumption, i.e., action is separate process from decision and starts only when the decision is made. However, many decisions take place within dynamic environments, in which individuals have to evaluate and compare the alternative options while acting. For instance, there are cases where people have to continuously explore novel environments and evaluate and compare the alternative options to make spatial decisions. Recent experimental studies proposed an “action-based” theory as an alternative framework to model decisions between actions. The core idea of this theory is that the selection between actions takes place within the same areas that plan and guide action execution through a continuous competition between populations of neurons associated with the alternative actions [11,12,18,75]. In particular, when the brain is faced with multiple potential goals (and therefore multiple potential actions to achieve these goals), it generates concurrently action plans that compete for selection, and uses online information accumulated while acting to bias the competition until a single goal is selected. The competition

is biased by decision variables that are encoded in higher cognitive regions, such as frontal cortical areas and basal ganglia, but sensorimotor regions are responsible for selecting the final action.

The “action-based” theory has received apparent support from neurophysiological studies which reported decision-related neural activity in cortical regions that are mainly involved in planning and generating actions. For instance, Glimcher and his colleagues designed a visual-saccadic decision making task, where the monkeys were free to choose between two targets presented simultaneously in both hemifields [60]. While animals performed the task, neuronal activity was recorded from lateral intraparietal (LIP) neurons. LIP is an area of parietal cortex that is thought to transform visual signals into eye movements. Surprisingly, they found that decision variables, such as expected gain and probability of reward, modulated the activity of the neurons in the LIP. This is actually one of the first studies which showed that sensorimotor areas are somehow involved in decision making. In the next years, many studies showed that decision variables, such as the expected gain/punishment, hazard rate, outcome probability and others, are correlated with neuronal activity in parietal and premotor brain areas, such as LIP [21, 60], frontal eye fields (FEF) [14], dorsal premotor cortex (PMd) [53] and the superior colliculus (SC) [3] in non-human primates.

Although these findings provide evidence that sensorimotor regions are causally involved in decision making, the advocates of “goods-based” theory argue against these findings claiming that neuronal activity in these regions is not necessarily “genuinely motor”, but instead is related to spatial attention. To establish whether these re-

gions are causally involved in decision making process, a series of studies temporarily perturbed these regions, via microstimulation or inactivation with GABA-A agonist agents, and observed the effects on the decision making process. For instance, Wilke and her colleagues inactivated the LIP area, while monkeys performed a visual-saccadic decision making task. Results showed that the LIP “lesion” did not impair animals’ ability to perform saccadic movements to targets presented either in the contralateral or the ipsilateral hemifield. However, it created a spatial decision bias towards the ipsilateral targets when the animal was free to select between two targets located in both hemifields [84]. These findings suggest that the animals exhibit a spatial decision bias reminiscent of extinction syndrome observed in patients with parietal lesions. Similar spatial decision bias has also been reported in other brain perturbation studies. In one of them, researchers inactivated intermediate layers of SC, while monkeys performed a visual search task [43]. Results showed that after inactivation, animals made fewer saccades to the targets in the affected zone.

The involvement of sensorimotor regions in decision-making should be not very surprising. Consider for instance how frequently people and animals make decisions between actions, such as choosing a route to get back home from work avoiding traffic. Overall, these studies suggest that both frontal and sensorimotor regions have a significant role in value-based decision-making. Even though the main goal of this thesis is to assess the neural mechanisms of spatial decisions, we believe that these two types of decision-making problems share many similar characteristics with spatial decision tasks, and thus, they may share similar neural mechanisms. For

instance, when people or animals explore their environment to make spatial decisions, such as find a path to reach a goal or explore city maps to find a restaurant, they have to evaluate and compare the alternative options to make a decision. Hence, extracting and processing information from the environment to evaluate and compare the alternative options seems to be a common process in both economic choices and spatial decisions.

1.5 Exploring small city maps to make spatial decisions

Despite the significant contributions of mentioned studies, little is known on what information people extract about spatial characteristics of the environment, and how this information is coded into the brain to make spatial decisions. Information from our environment comes not only directly from experiencing the world like walking, but also indirectly from descriptions and depictions of the world [7, 78]. For instance, spatial representations can be derived through static images like pictures, photos, and maps. Humans have long recognized the importance and value of maps to their lives. Indeed, the history of mapping can be traced to more than 5,000 years ago, and either from stone, clay, wood, or paper maps have been invented by many cultures [6]. Nowadays, the exploration of city maps has exploded due to the wide availability and increased use of small, hand-held positioning and navigational devices.

City maps represent visual abstractions of urban areas with different geographic entities, their locations, and spatial relations. Investigating key parameters of the maps can provide promising access to the way humans perceive, represent, and interact with their spatial environment. This is the ultimate goal of this thesis. We are interested in understanding the neural mechanisms of visual exploration and choice destination in real city maps. We address the question of whether and how features of special importance for map exploration are encoded in the brain, during a visual exploration task for making decisions (Chapter 2). We are also interested in understanding how people explore novel environments to make spatial decisions in a forced-choice (also known as instructed-choice) task, i.e., people have to choose an option from a “choice menu” (Chapter 3).

1.5.1 Spatial characteristics of city maps

Spatial characteristics of maps can be quantified using space syntax, a set of analytic techniques that are used to describe the intrinsic spatial structure of a street network by measuring the relationship of each part to all others [27, 58],

In this framework, street networks are described by measures of their average properties over an area: street length per unit area, number of intersections and number of dead ends per unit area, and average distance between intersections. These measures describe sub-areas of a map, and are not sufficient for the analysis of actual or virtual navigation in maps. Space syntax measures have been correlated to the distribution

of pedestrian movement over an urban area [28–30, 56, 57], to the legibility of urban areas (i.e., ‘image’ of an urban area can be categorized into paths, edges, nodes, and landmarks) [54], and to navigation choices in virtual urban environments [15]. Due to its ability to model aspects of urban legibility, navigation and functionality, space syntax is being applied to the evaluation of urban designs.

A recent study explored the behavioral mechanisms underlying map exploration [10]. In particular, Christova and her colleagues conducted a psychophysical experiment to study gaze behavior during exploration of small city maps. Subjects had to explore by eyes city maps of different street network layouts, in order to select a location to build a hypothetical City Hall. The results showed that people chose City Hall locations with very similar space syntax attributes. In particular, they selected the most accessible location. Accessibility was assessed by two space syntax measures, namely, directional reach and metric reach [55]. Directional reach is a measure of the total street length available within a specified number of direction changes, whereas metric reach shows how much total street length is available within a walking distance. These findings suggest that map exploration is a rich process involving space syntax attributes.

1.5.2 Neural mechanisms underlying exploration of city maps and choice of destination

The neural mechanisms underlying spatial cognition in the context of exploring realistic city maps are unknown. Previous studies suggest that people use spatial information to make decisions [10, 17]. Part of this thesis (Chapter 2) focuses on understanding the neural mechanisms underlying this behavior. In particular, we are interested in understanding whether and how the brain encodes spatial information (i.e., map characteristics) in visual exploration tasks that can be used to evaluate the alternative options and make decisions (e.g., find a place to build a landmark). To address this question, we conducted a novel brain imaging experiment, in which participants were asked to explore small city maps exemplifying different street network types, in order to select a location to build a hypothetical City Hall. Neural activity was recorded using a 248-sensors whole-head axial MEG system at high temporal resolution. We locally characterized each of the city maps by computing 3 space syntax attributes within an area centered on each eye fixation location (i.e., the area around each fixation that subjects presumably covertly explored to decide where to look next): i) total street length, ii) number of street intersections, and iii) regularity index, which measures the degree to which the distribution of the street intersections deviates from complete spatial randomness to either clustering or regularity [13].

The following describe briefly our main findings (see Chapter 2 for more details). Analyzing the association between neural activity and space syntax parameters, re-

vealed brain areas whose neural activity was strongly related with these parameters. These areas were mostly localized in the right frontal and prefrontal areas of the brain, suggesting that these regions may have an important role in encoding spatial information for decision making. We also found other areas that were involved in the processing of space syntax parameters, such as parieto-occipital cortex, cerebellum, and right temporal areas. Importantly, we showed that processing of space syntax parameters depends on the map type (i.e, street network type). In particular, for some types of street network there was stronger association between neural activity and space syntax parameters than other map types. This finding suggests that depending on the map type people may use different kinds of spatial information to make decisions. Hence, when the association between neural activity and space syntax parameters was strong, it is likely that subjects used mostly these spatial parameters as decision variables, - in the sense that space syntax parameters were used for the evaluation of the “attractiveness” of a location-, to evaluate and compare the alternative locations. On the contrary, when the association was weak, people seem to possibly use other spatial features of the maps, besides these space syntax parameters, to select the City Hall location.

1.5.3 Behavioral mechanisms underlying spatial decisions with instructed-choices

In the task described above (section 1.5.2) people were free to choose any location to build the hypothetical City Hall. However, we frequently make decisions between options from a “menu-choice”. In other words, we usually have to select between a limited number of options, e.g., a governor selects between particular options to build a new stadium, city hall, post-office, etc. In Chapter 3 we focus on understanding how people change their exploration and decision making strategies, when we limit their choices. To address this question we designed a psychophysical experiment similar to map exploration task of Chapter 1, but now subjects had to select between two alternative locations marked on the map to build a hypothetical Post Office.

The following describe briefly our main findings (see Chapter 3 for more details). Analyzing subjects’ eye positions during map exploration revealed that people adopted similar strategies with value-based decisions [35, 36] and way-finding tasks [9, 17]. In particular, subjects spent more time exploring around the option they finally selected. Also, initial fixations around an option favored the location ultimately chosen. Finally, subjects were exploring the areas around the two alternative locations and the center of the map by looking repeatedly back and forth between them. This was actually one of the main differences between our experiment and value-based decisions. In particular, people are looking repeatedly between the alternative items/stimuli in economic choices, presumably implementing a compari-

son process between them [35, 36]. However, in our study people spent a significant amount of time to also explore the area around the center of the map. We discussed more about this interesting finding in Chapter 3, but we can briefly mention here that people may have followed this strategy to compare the two alternative locations with respect to the center of the map, assuming that this was their current location. This argument is strengthened if you consider that subjects had to select the Post Office location by moving a cursor located at the center of the map to the selected point.

Chapter 2

Neural mechanisms underlying the exploration of small city maps using magnetoencephalography

2.1 Overview

The neural mechanisms underlying spatial cognition in the context of exploring realistic city maps are unknown. We conducted a novel brain imaging study to address the question of whether and how features of special importance for map exploration are encoded in the brain to make a spatial decision. Particularly, subjects explored by eyes small city maps exemplifying five different street network types in order to locate a hypothetical city hall, while neural activity was recorded continuously by 248 magnetoencephalography sensors at high temporal resolution. Monitoring subjects'

eye positions, we locally characterized the maps by computing three space syntax parameters of the areas that were explored. Particularly, we computed the number of street intersections, the total street length, and the regularity index in the circular areas of 6 degrees of visual angle (DVA) radius centered on instantaneous eye positions. We tested the hypothesis that neural activity during exploration is associated with space syntax parameters and modulated by street network type. All time series were rendered stationary and non-autocorrelated by applying an autoregressive integrated moving average model and taking the residuals. We then assessed the associations between the prewhitened time-varying MEG time series from 248 sensors and prewhitened space syntax parameters time series, for each street network type, using multivariate multilinear regression analyses. In accord with our hypothesis, ongoing neural activity was strongly associated with space syntax parameters through localized and distributed networks, and neural processing of these parameters depended on the type of street network. Overall, processing of space syntax parameters seems to predominantly involve right frontal and prefrontal areas, but not for all street network layouts. These results are in line with findings from a series of previous studies showing that frontal and prefrontal areas are involved in processing of spatial information and decision making. Modulation of neural processing of space syntax parameters by street network type suggests that some street network layouts may contain other types of spatial information that subjects use to explore maps and make spatial decisions.

2.2 Introduction

The ability to make spatial decisions while exploring an environment is a fundamental component of human and animal behavior and very critical for survival. For instance, animals in nature explore their surroundings to obtain food, avoid predators, and find mates. Similarly, people frequently explore new environments to find places for food and entertainment, buy new houses, etc. Nearly all these problems involve some aspects of spatial information processing in which humans/animals extract spatial information from the environment to combine it with other decision variables, internal states (e.g., hunger level) and external states (e.g., threat level) to make decisions. The question of how people and animals extract and process spatial information for making decisions is a topic of many ongoing studies.

For years, scientists have strived to understand how we interact with our environment to collect information required to make decisions or to select actions. One of the studies that aimed to address this question involved a maze solving task [17], in which individuals were presented with a maze stimulus on a video display and had to indicate which of several possible exits from the maze was continuous with a specific entrance. The hypothesis was that the reaction time of a correct decision would depend on spatial characteristics of the exiting route. Consistent with this hypothesis, results showed that reaction time was positively correlated (i.e., increased) with the length of the main path, the number of turns in the path, and the direct distance from the entry to the end-point. Additionally, gaze behavior and eye fixations were

also modulated by spatial characteristics of the mazes. In particular, the number of fixations increased as a function of path length and number of turns, and the eyes tended to fixate on the main path and follow it along its main course. Note that similar results were reported in a maze solving experiment with non-human primates [9]. All these findings suggest that: i) people and animals can solve mazes in a similar fashion, ii) the postulated dynamic spatial process involves a mental tracing of the maze path, and iii) a significant aspect of the spatial information processing involves the length and turns of the path.

While these studies provide important knowledge on which and how spatial information is processed during exploration tasks, mazes were randomly generated and restricted. A recent study extended the maze solving task using small city maps as stimuli [10]. The advantage of this approach was that city maps are rich networks of straight and/or curved streets, and clearly people are more familiar in exploring city maps than mazes. According to this study, people had to explore continuously realistic small city maps of various U.S. cities by moving their eyes, in order to select a location to build a hypothetical City Hall. Unlike the maze solving task, this study involved both exploration and spatial decision making. Hence, people had to collect spatial information not to find a path to a goal, but to identify a location for building the City Hall. Results showed that people chose City Hall locations with very similar space syntax attributes. In particular, they selected the most accessible places compared to the average city map.

All these findings suggest that people and animals use particular spatial infor-

mation from the environment to solve spatial-context problems and make decisions. However, little is known about the neural mechanisms underlying spatial information processing. In the current study, we aim to address the question of how the brain encodes spatial information while humans explore novel environments to make spatial-decisions. To do that, we conducted a novel brain imaging experiment, in which subjects were instructed to explore by eyes various U.S. city maps exemplifying five different street network types, i.e., regular, colliding, curvilinear, cul-de-sac, and supergrid, in order to select a location to build a hypothetical City Hall. We recorded neuromagnetic fluxes from subjects' heads using a 248-sensor whole-head magnetoencephalography device. We also monitored subjects' eye positions to locally characterize the maps by computing three space syntax attributes in the circular area of 6 DVA radius centered on each eye position (i.e., covertly explore area): a) total street length, b) number of street intersections, and c) regularity index that measures the degree to which the distribution of street intersections deviates from complete spatial randomness to either clustering or regularity.

The original hypothesis was that some or all of these space syntax parameters are encoded in the brain through characteristic neuronal networks, and neural processing of these parameters is modulated by street network type. We used Box-Jenkins time series analysis [5] to remove confounding autocorrelations and trends from both MEG raw data and space syntax parameters time series (prewhitening). After obtaining quasi-stationary time series, we assessed the relation between the time varying MEG signal from the 248 sensors with the variability of each of the space syntax parameters,

for each street network type, using multivariate multiple linear regression analyses. In accord with our initial hypothesis, ongoing neural activity was strongly associated with space syntax parameters through localized and distributed networks, and the neural processing of these parameters was modulated by the type of street network.

In particular, processing of space syntax parameters seems to predominantly involve right frontal and prefrontal areas, but not for all street network layouts. Particularly, neural processing of the number of street intersections and total street length was involved mainly in regular, colliding, and curvilinear grids, whereas the rest of the street network types were not involved in the processing of these space syntax characteristics. This finding suggests that the number of street intersections and the total street length may not be such important features for map exploration and spatial decisions for cul-de-sacs and supergrids, as for regular, colliding, and curvilinear grids. Similarly, cul-de-sacs, supergrids, and curvilinear grids involved minimal processing of the regularity index, implying that these street network layouts may contain other type of information, besides the regularity index, that subjects used to explore the maps and make spatial decisions. To the best of our knowledge, this is the first study showing that brain encodes spatial information through particular neuronal networks.

2.3 Materials and methods

2.3.1 Participants

Ten right-handed subjects (5 women and 5 men) participated in the study for monetary compensation. Subjects' age ranged from 23 to 41 years. The appropriate Institutional Review Board approved the study protocol, and the informed consent was obtained from all the participants based on the Declaration of Helsinki.

2.3.2 Stimuli

The stimuli used in this task, are the same stimuli used in a previous study conducted in our laboratory [10]. Stimuli are circular maps of 3-mile diameter urban areas extracted from street center-line maps and represent several U.S. Metropolitan Statistical Areas (Atlanta, GA; Baltimore, MD; Chicago, IL; Los Angeles, CA; New York, NY; Pittsburgh, PA; St. Louis, MO; Tampa, FL; Washington, DC). Street center-line maps show information only about the position of the streets relative to one another, scaled length, alignment, sinuosity and pattern of intersections of the street network, and do not feature scaled street width, topography, urban development and land use, or any other 3-dimensional information. Therefore, the choice of stimuli is based on studying how subjects respond to the spatial structure of the street network, and particularly its shape, density and connectivity.

The sample was chosen to represent five ideal types of street networks: (i) *regular grids*, that consist of orthogonally intersecting patterns of streets, (ii) *colliding grids*,

that arise from the intersection of multiple regular grids rotated with respect to one another, (iii) *curvilinear grids*, that arise from the intersection of curvilinear streets, (iv) *cul-de-sacs*, that consist of hierarchically branching street networks encompassing many cul-de-sacs, and (v) *supergrids*, that consist of sparsely spaced orthogonally intersecting main arteries with irregular street patterns filling-in the large blocks surrounded by the arteries.

Four stimuli per street network type (all together 20 stimuli) were presented to each subject in a pseudorandom sequence, Fig. 2.1.

2.3.3 Experimental Paradigm

Task

A trial started with subjects fixating their eyes in an open circle presented at the center of a black screen, and positioning an x - y joystick cursor inside the circle using their right hand. After 1.5 s, the stimulus appeared and subjects were asked to choose a hypothetical City Hall location by clicking in the desired location. Subjects were instructed to hold the joystick cursor at the center until deciding on the City Hall Location, and experiment proceeded at subjects' pace, Fig. 2.2.

Experimental Setup

The task stimuli were generated by a computer and were presented on a display 62 cm in front of the subjects, using a Liquid Crystal Display (LCD) projector and a

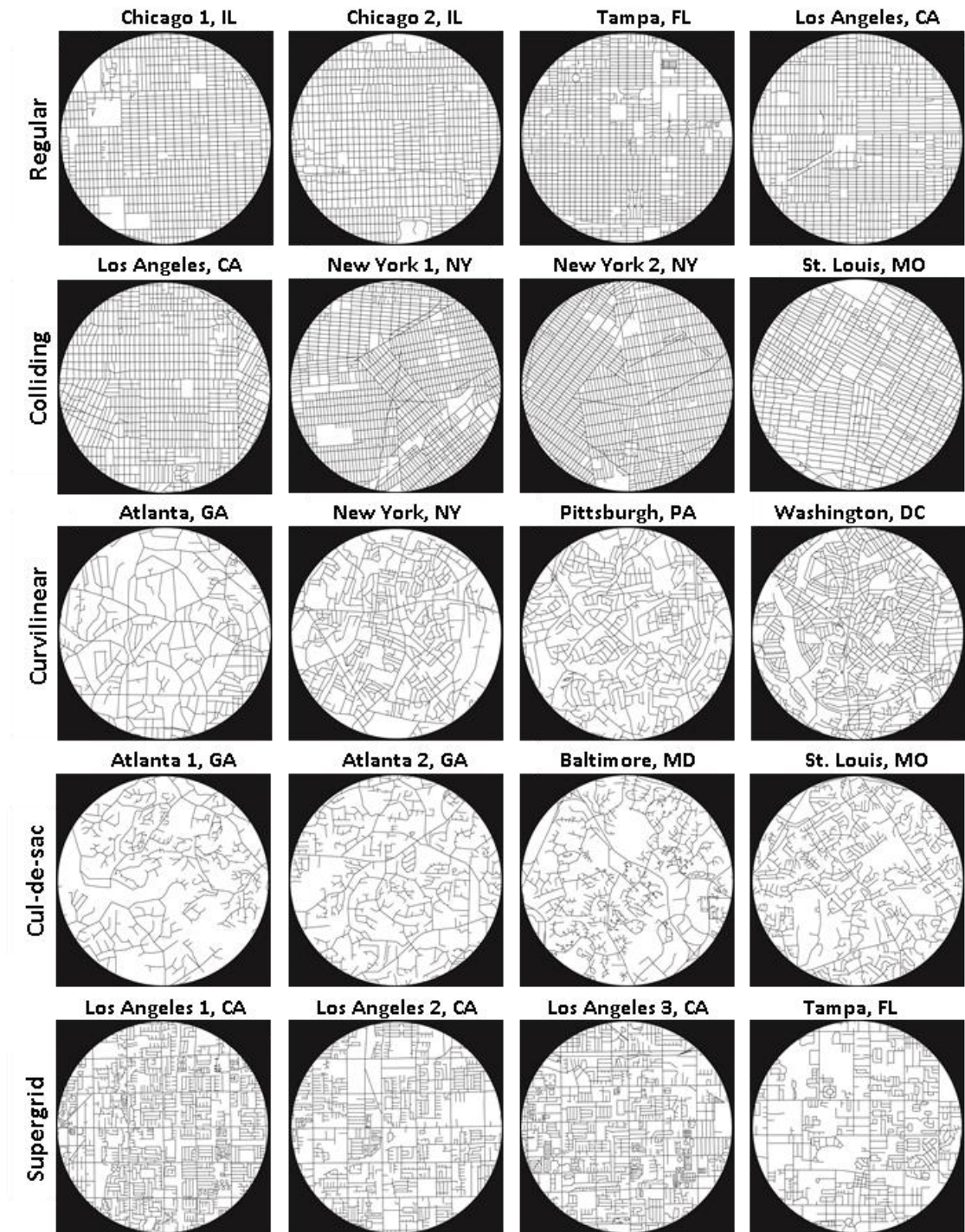


Figure 2.1: Map stimuli. Each row corresponds to stimuli of the same street network type. There are totally 20 stimuli, 4 stimuli per street network type.

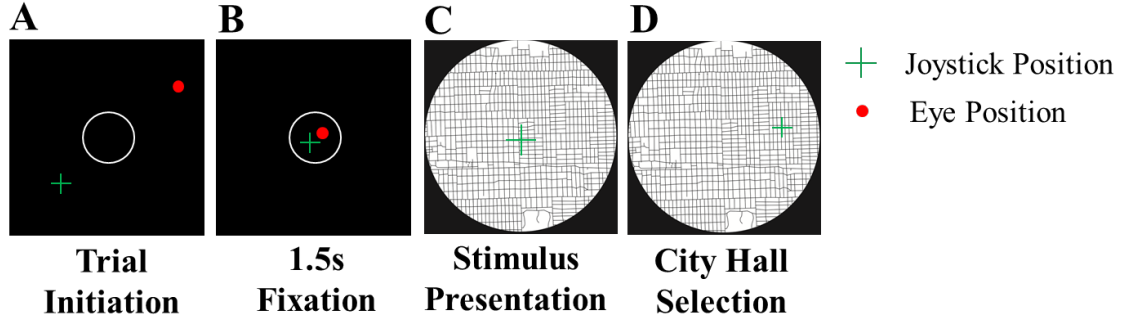


Figure 2.2: Task sequence. (A) Trial starts with the presentation of an open circle on the center of a black screen. (B) The subject is required to fixate eyes and place the mouse inside the circle for 1.5 s. (C) The stimulus is presented and subject explores the map by moving his/her eyes in order to decide where to place a hypothetical City Hall. (D) The subject chooses the City Hall location by clicking the mouse at the desired position.

periscopic mirror system. The stimuli displayed subtended approximately 10 degrees of visual angle. Subjects lay supine in the recording chamber having their head inside the cryogenic helmet-shaped dewar, Fig.2.3 (left panel). During the task, subjects were using a 2D joystick (joystick model: 541 FP, Measurement Systems, Norwalk, CT; remodeled by removing all the magnetic parts). The joystick was placed on the resting bed, next to subjects' right hand.

2.3.4 Data acquisition

The experiment was controlled by a program written in Visual basic (Microsoft Visual Basic 2005, version 8.0). Relevant data include the times of presentation of stimuli, the x - y position of the mouse (updated at 200 Hz and collected at 1017 Hz), the x - y position of the eyes (updated at 60 Hz and collected at 1017 Hz), and the MEG signals from 248 sensors (collected at 1017 Hz). The eye position was recorded using

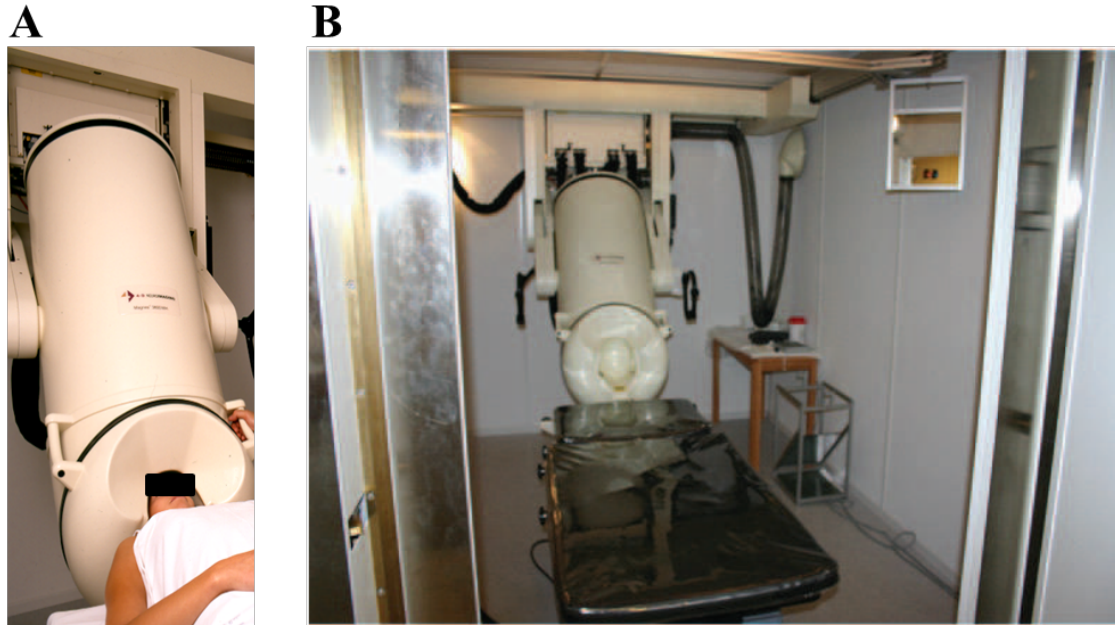


Figure 2.3: **(A)** Subject lays supine in the recording chamber with head inside the cryogenic helmet-shaped dewar. **(B)** The 248-sensor whole-head MEG system is located inside a shielded room that reduces electromagnetic and environmental noise.

a nonmagnetic video-based pupil/corneal reflection tracing system (model EGL-400, ISCAN, Inc. Burlington, MA).

Magnetoencephalography

Brain activity was recorded using a 248-sensors whole-head axial MEG system (Magnes 3600 WH, 4-D Neuroimaging, San Diego, CA), Fig. 2.4. The cryogenic helmet-shaped dewar of the MEG system was located inside a shielded room that reduced electromagnetic and environmental noise, Fig.2.3 (right panel). The MEG data were recorded at 1017.25 Hz and filtered down to 0.1-400 Hz during acquisition.

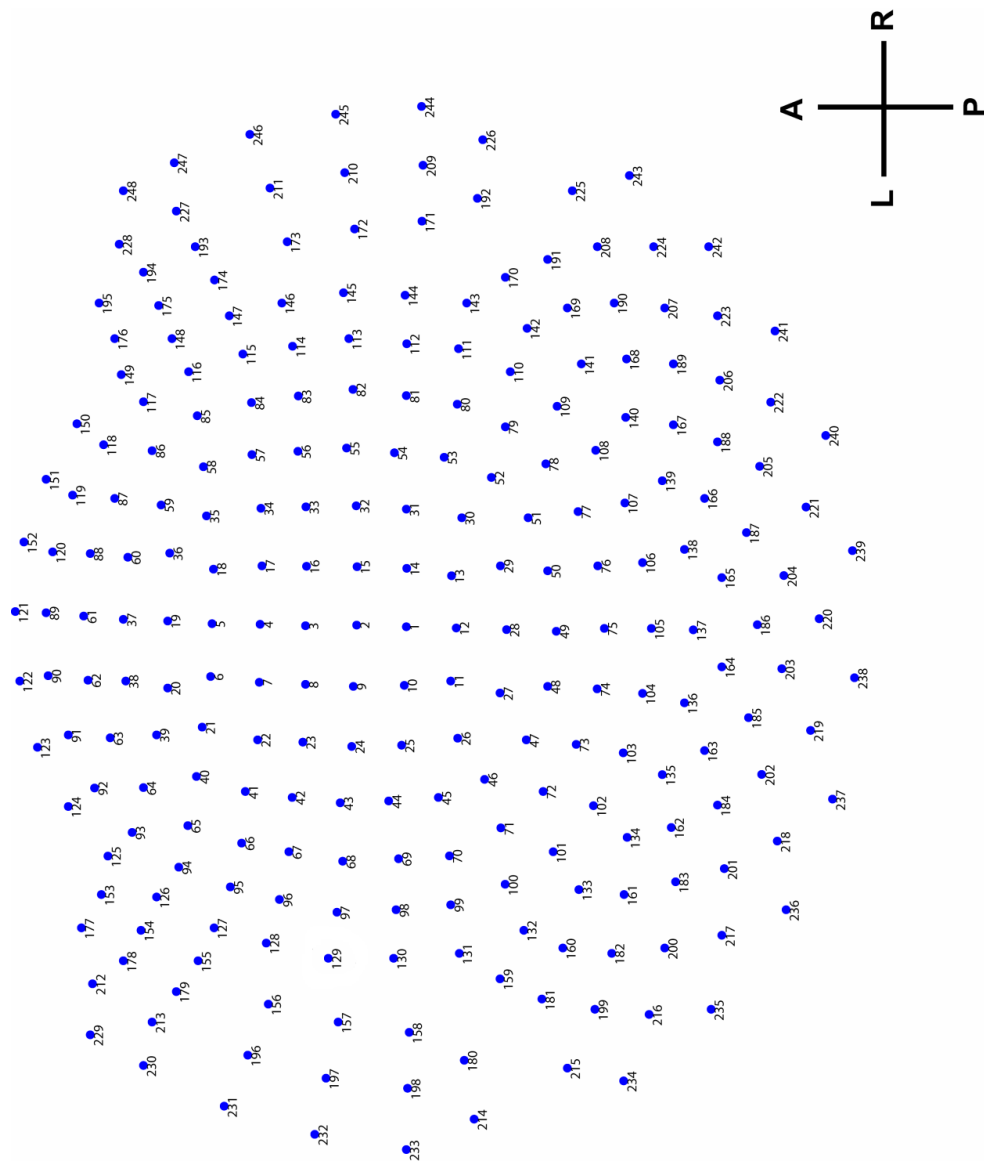


Figure 2.4: 2D projection of the 248-channel axial gradiometer MEG system used to record brain activity.

2.3.5 Data preprocessing

The obtrusive cardiac artifact was removed from the MEG data using the event-synchronous subtraction method [38]. MEG recordings were downsampled by averaging the MEG time series every ~ 16.7 ms to align them with eye position recordings.

2.3.6 Time series analysis

Neurophysiological time series often are not stationary with respect to their mean and variance, and in many cases are dominated by trends which should be recognized before any analysis of correlation between time series is done. Without removing nonstationarities from the data spurious associations could arise [5, 33, 39]. Since the main goal of this study was to assess the associations between MEG time series and map parameters, the data should be stationary. Therefore, we used an autoregressive integrated moving average (ARIMA) model to render the recorded MEG data stationary and nonautocorrelated. The autoregressive (AR) model eliminates any linear dependencies (i.e., autocorrelations) within the individual time series, the integrated factor (I) differentiates the time series to remove possible linear trends, and the moving average (MA) model smoothes the time series by taking the weighted linear summation of random shocks (i.e., noise terms). Based on previous MEG studies [37, 39], an ARIMA(25,1,1) model was adequate to obtain quasi-stationary time series (i.e., ‘prewhitened’ data).

2.3.7 Map Parameters

The whole map was analyzed and characterized by the street network type (i.e., regular grid, colliding grid, curvilinear grid, cul-de-sacs, supergrid), and parts of the map defined by the circular areas of radius 6 degrees of visual angle centered on each $x-y$ eye positions (i.e., covertly explored areas), Fig.2.5, were analyzed by three space syntax attributes. The first two measures comprise the *Total Street Length per unit area* and the *Number of Street Intersections per unit area* within the circular areas of radius 6 DVA centered on instantaneous $x-y$ eye position. The third measure is the *Regularity Index* within the circular areas of radius 6 DVA centered on instantaneous $x-y$ eye positions.

Regularity index is a measure of the degree to which a given point distribution deviates from complete spatial randomness to either clustering or regularity. In a random distribution of a set of points on a given area, it is assumed that any point has had the same chance of occurring on any sub-area as any other point, that any sub-area of specified size has had the same chance of receiving a point as any other sub-area of that size, and that the placement of each point has not influenced by than of any other point [13].

The basis for this measure of spacing is given by the distance from an individual to its nearest neighbor, irrespective of direction. For a set of n points where the distance between the i th and the j th point is u_{ij} , the observed mean nearest neighbor

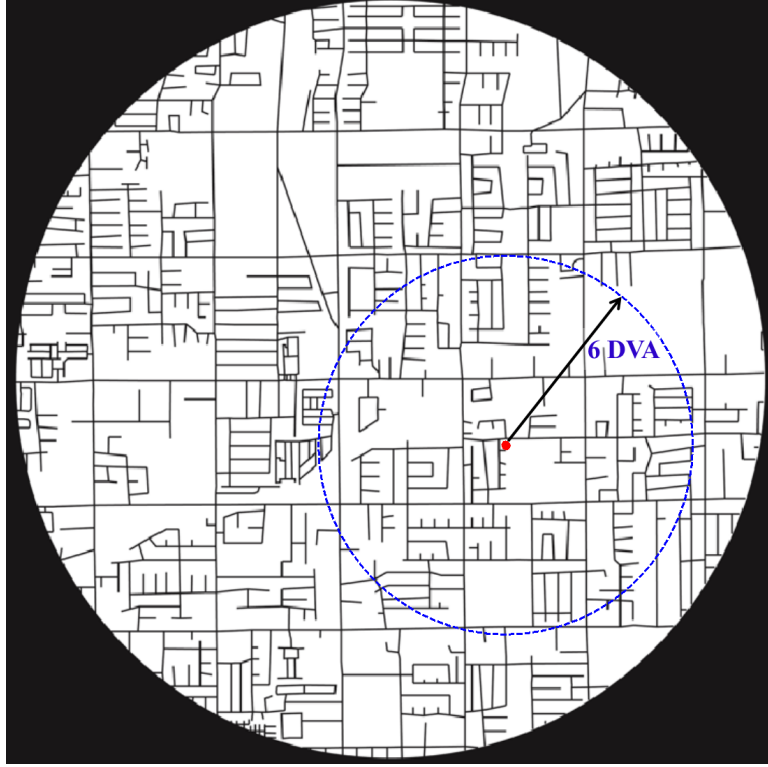


Figure 2.5: Parts of the map defined by the circular areas of 6 degrees of visual angle radius centered on instantaneous $x-y$ eye positions were analyzed by space syntax characteristics. The red dot marks an eye fixation on the map, and blue circle corresponds to the circular area of 6 DVA radius centered on this eye position.

distance is, Eq. (2.1),

$$\bar{r}_A = \frac{1}{n} \sum_{i \neq j}^n \min\{u_{ij}\} \quad (2.1)$$

In our case, the n points correspond to the street intersections within the circular areas of 6 DVA radius centered on instantaneous $x-y$ eye positions. We also calculated the mean distance to nearest neighbor that would be expected if the individuals of that population were randomly distributed. Complete spatial randomness for n points in an area A , assuming that a point is equally likely to fall at each location in the area,

and that multiple points are chosen independently, is described by the Poisson process, in which the probability density function for the nearest neighbor distance d and point density $\rho = \frac{n}{A}$ (i.e., the mean number of points per unit area), is $p(d) = 2\pi\rho d e^{-2\pi\rho d^2}$. The expectation of this distribution (i.e., mean distance between nearest neighbors for a random process) can be shown to have a value equal to Eq. (2.2) [13].

$$\bar{r}_E = \frac{1}{2\sqrt{\rho}} \quad (2.2)$$

The ratio of the observed mean distance to the expected mean distance is the Regularity Index, Eq. (2.3),

$$R = \frac{\bar{r}_A}{\bar{r}_E} \quad (2.3)$$

and serves as a measure of the degree to which the observed distribution approaches or departs from random expectation. Particularly, under this approach, clustering, randomness, and regularity are conceptualized as laying along a continuum. In a random distribution $R = 1$. Under conditions of maximum aggregation all points are superposed, and therefore, $R = 0$. Under conditions of maximum spacing, the points are spaced with perfect uniformity, as in triangular lattice arrangements, and R will have the value of $R = \frac{1.0746}{\sqrt{\rho}} = 2.1491$ [13].

2.3.8 Analysis of the relations between neural activity and map parameters

Our initial hypothesis was that the ongoing neural activity is associated with some or all space syntax parameters. To test that, we performed multivariate multiple linear regressions, one for each space syntax parameter, where the prewhitened time-varying MEG signal from 248 sensors was the dependent variable, and the independent variables were: a) a space syntax parameter time series (i.e., number of street intersections or total street length or regularity index), b) the x eye position time series, and c) the y eye position time series. However, we found that space syntax parameters time series were not stationary. Following the same procedure with neural data, we used an ARIMA model to remove the autocorrelation structure from space syntax parameters time series. After extensive ARIMA modeling and diagnostic checking including the computation and evaluation of the autocorrelation (ACF) and the partial autocorrelation functions (PACF) of the residuals, we found that ARIMA(25,1,1) was adequate to yield quasi-stationary time series. Finally, we prewhitened the independent nuisance variables, x - y eye position time series, using also an ARIMA(25,1,1) model.

After all times series were rendered stationary and nonautocorrelated, we performed 3 multivariate multiple linear regressions, one for each space syntax parameter,

Eq. (2.4)-(2.6).

$$Y_{n \times 248} = \mathbf{StrIntersect}_{n \times 1} a_{1 \times 248} + \mathbf{Xeye}_{n \times 1} k_{1 \times 248} + \mathbf{Yeye}_{n \times 1} l_{1 \times 248} + E_{n \times 248} \quad (2.4)$$

$$Y_{n \times 248} = \mathbf{StrLength}_{n \times 1} b_{1 \times 248} + \mathbf{Xeye}_{n \times 1} k_{1 \times 248} + \mathbf{Yeye}_{n \times 1} l_{1 \times 248} + E_{n \times 248} \quad (2.5)$$

$$Y_{n \times 248} = \mathbf{RegIndex}_{n \times 1} c_{1 \times 248} + \mathbf{Xeye}_{n \times 1} k_{1 \times 248} + \mathbf{Yeye}_{n \times 1} l_{1 \times 248} + E_{n \times 248} \quad (2.6)$$

Y is the dependent variable matrix with columns consisting of the 248 MEG prewhitened time series of size n . **StrIntersect**, **StrLength**, **RegIndex**, **Xeye** and **Yeye** are the prewhitened independent variables time series, and a , b , c , k , and l the corresponding regression coefficients. Finally, E is the error matrix.

To also assess whether the neural processing of space syntax parameters is modulated by the type of street network we performed the same regressions, Eq. (2.4)-(2.6), for each street network layout, i.e., regular, colliding, curvilinear, cul-de-sac, and supergrid.

The relations of the brain signals with the space syntax parameters were quantified and summarized using the absolute t -values corresponding to the regression coefficients of the regressions, Eq. (2.4)-(2.6). The absolute value of the regression coefficient indicates the strength of the relation, whereas its associated t -value (i.e., ratio of the mean regression sum of squares divided by the mean error sum of squares)

is a measure of the significance of the regression. Specifically, when running a regression, we are trying to discover whether the coefficients on independent variables are really different from 0 (so the independent variables are having a genuine effect on your dependent variable) or if alternatively any apparent differences from 0 are just due to random chance. The t statistic is the coefficient divided by its standard error. The standard error is an estimate of the standard deviation of the coefficient, the amount it varies across cases. It can be thought of as a measure of the precision with which the regression coefficient is measured. If a coefficient is large compared to its standard error, then it is probably different from 0.

Comparison of brain maps

Overall, the regression analyses revealed significant relations between the ongoing MEG activity and space syntax parameters. We were interested in comparing the neural processing of these parameters between street network layouts, in other words, to get a measure of how similar two spatial distributions are, particularly, the spatial distributions in the MEG sensor space of the t -values corresponding to a space syntax parameter for two different grids. We calculated the root-mean-square (RMS) value of the difference between the absolute t -values corresponding to a space syntax parameter k for each pair of grids (i, j) , Eq. (2.7),

$$\mathbf{RMS}_k(\text{grid} = i, \text{grid} = j) = \sqrt{\frac{\sum_{s=1}^{248} (|\mathbf{tval}_{i,s}| - |\mathbf{tval}_{j,s}|)^2}{248}} \quad (2.7)$$

where k corresponds to a space syntax parameter (i.e., number of street intersections, total street length, and regularity index), *grid* is the street network type (i.e., regular, colliding, curvilinear, cul-de-sac, and supergrid), and s the MEG sensor number. \mathbf{RMS}_k is a 5×5 distance matrix, with entry (i, j) corresponding to the “similarity” of the spatial distributions in the sensor space of the t -values for space syntax parameter k between grids i and j .

Distances between objects can be visualized in many simple and evocative ways. Here, we are considering a graphical representation of a matrix of distances or dissimilarities (in our case the RMS matrix) with a dendrogram or a tree, where the objects are joined together in a hierarchical fashion from the closest, that is most similar, to the furthest apart, that is the most different. Hierarchical clustering analysis of n objects is defined by a stepwise algorithm which merges two objects at each step, the two of which have the least dissimilarity. At each step, the matrix of dissimilarities is updated by the average dissimilarity of the between-cluster dissimilarities (average linkage). The result of the hierarchical clustering analysis is a binary tree, or dendrogram, with $n-1$ nodes. In hierarchical tree clustering, clusters are distanced from an origin according to a scaling factor starting at distance 0 for items that are approximately equal and ending at distance 25 for items that are very different. Therefore, the further from the origin a cluster forms, the less alike they can be considered.

2.4 Results

2.4.1 Prewhitening neural data

We started the time series analysis by evaluating the stationarity of the raw data. Fig. 2.6 displays the MEG signal from sensor 1 (subject 2), before and after applying the ARIMA(25,1,1) model. Before the model was applied, the raw series were not stationary with respect to their mean and standard deviation. However, the non-stationarity was significantly reduced after applying the ARIMA model. In addition,

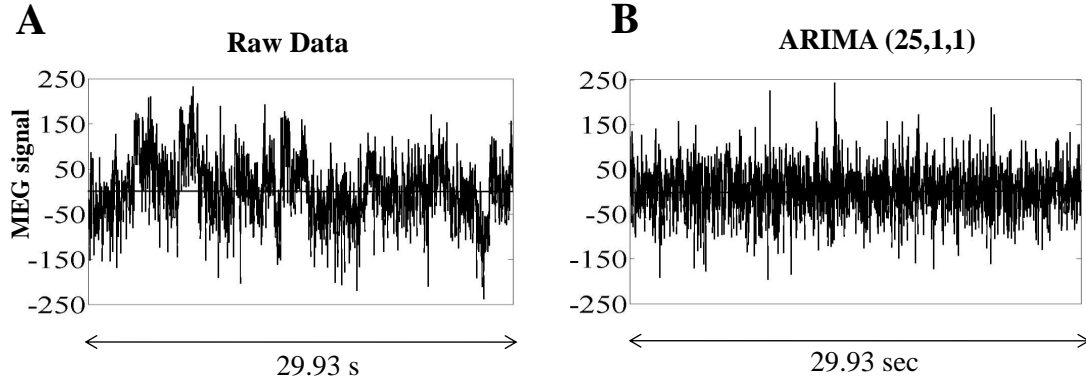


Figure 2.6: Subject 2 MEG raw data (29.93 s for 20 trials) from sensor 1 (**A**) before and (**B**) after applying ARIMA(25,1,1) modeling.

Fig. 2.7 (A and C panels) displays the autocorrelation function (ACF) and the partial autocorrelation function (PACF) of the raw MEG data recorded from sensor 1 from the same subject. The structure of ACFs and PACFs indicate that raw data are not stationary with respect to their autocorrelation. However, after applying ARIMA model, ACFs and PACFs became flat, indicating that the prewhitened data (i.e., ARIMA residuals) are also stationary with respect to their autocorrelations, Fig. 2.7

(B and D panels) (see [39] for further information about time series analysis in MEG data).

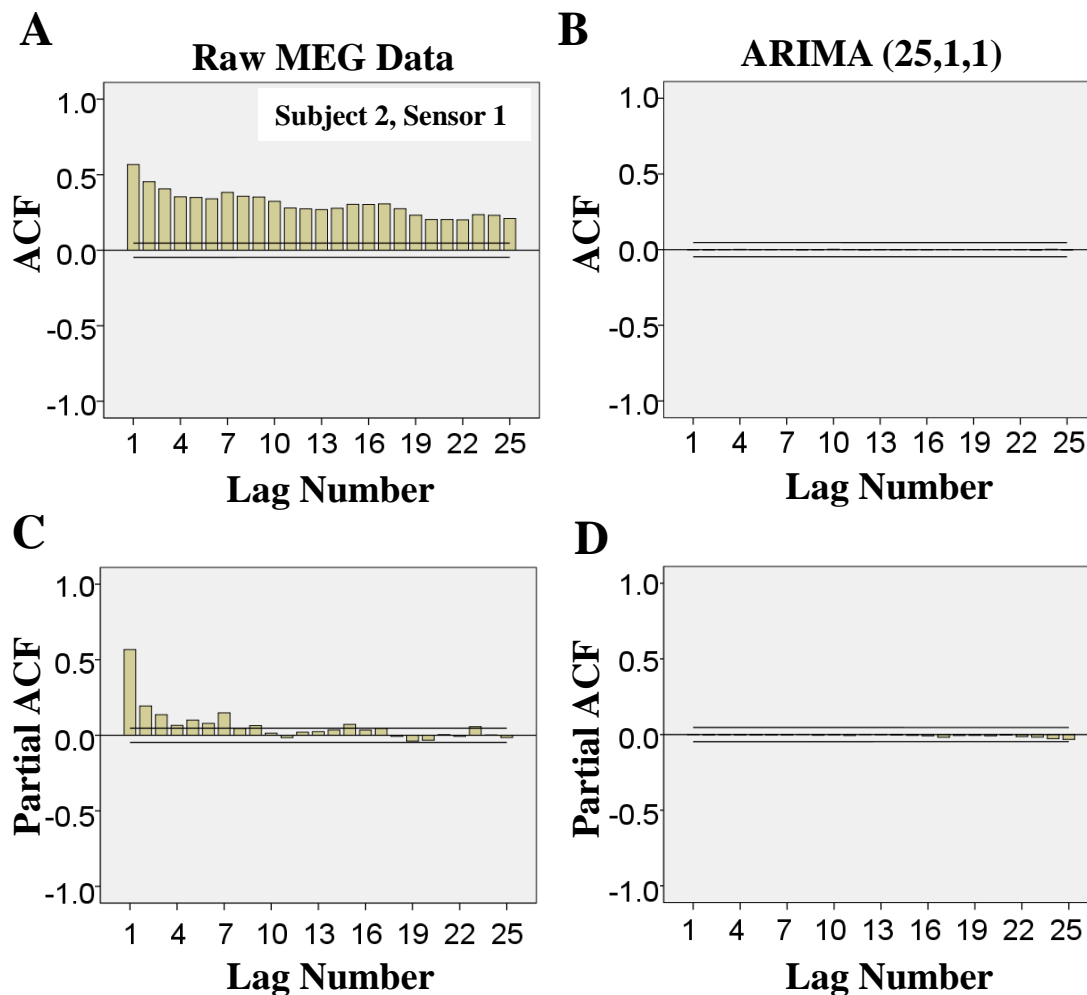


Figure 2.7: ACF structure of the MEG signal recorded from sensor 1 (subject 2) before (A) and after (B) applying an ARIMA(25,1,1) model. PACF structure of the MEG signals recorded from the same sensor before (C) and after (D) applying the model. The black lines that are close to the reference zero-line, denote 95% statistical significance level from the ACF and PACF value. Notice that the strong autocorrelation and partial-autocorrelation structure on the raw data disappeared after applying ARIMA(25,1,1) modeling. That is, the ACFs and PACFs are flat.

2.4.2 Map parameters

While exploring the maps, subjects fixated their eyes at various locations. For each $x-y$ eye position, we computed three attributes that describe locally the map, particularly, the circular area of radius of 6 degrees of visual angle centered on the eye position. We refer to them as *space syntax parameters*, and they are the number of street intersections, the total street length and the regularity index within the circular areas of 6 DVA radius centered on instantaneous $x-y$ eye positions. We then evaluated the stationarity of these space syntax parameters time series. Figs. 2.8, 2.9 and 2.10 present the autocorrelation and the partial autocorrelation function of the number of street intersections, the total street length, and the regularity index respectively. The structure of both ACF and PACF indicates that space syntax parameters time series are not stationary. However, ACF and PACF became flat after applying ARIMA(25,1,1) model, indicating that the prewhitened data are stationary, Figs. 2.8, 2.9 and 2.10 (panels B and D).

Maps are characterized globally by the spatial structure of the street network, that is the street network type. Tables 2.1- 2.5 summarize for each street network type (regular, colliding, curvilinear, cul-de-sac, and supergrid respectively) some of the basic statistics of the space syntax parameters for each subject. Fig. 2.11 illustrates the mean of number of street intersections (panel A), total street length (panel B), and regularity index (panel C) across subjects for each street network type. Note that for the same street network type the variability of space syntax parameters among

subjects is low. However, space syntax parameters vary significantly across grids ($P < 0.0001$). On the other hand, exploration time did not depend on the street network type ($F = 0.172$, $P = 0.952$).

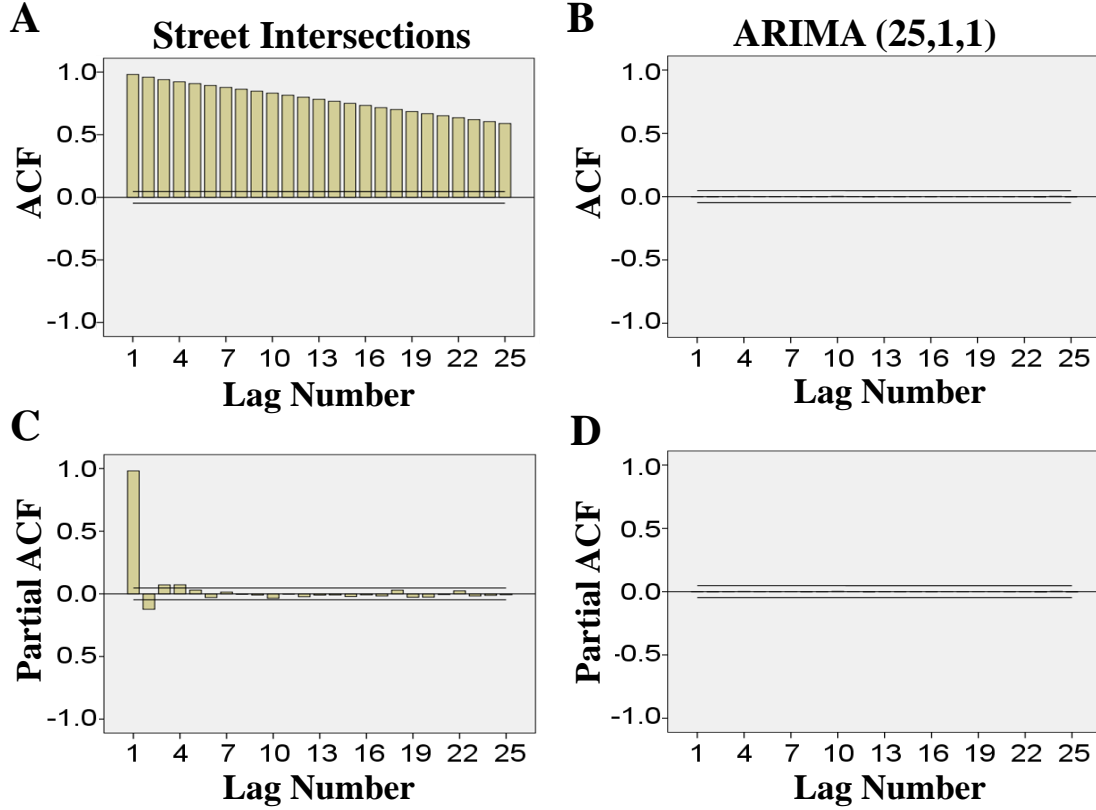


Figure 2.8: ACF structure of number of street intersections from subject 2 before (A) and after (B) applying an ARIMA(25,1,1) model. PACF structure of number of street intersections recorded from the same subject before (C) and after (D) applying the model. The black lines that are close to the reference zero-line, denote 95% statistical significance level from the ACF and PACF value. Notice that the strong autocorrelation and partial-autocorrelation structure on the raw data disappeared after applying ARIMA(25,1,1) modeling. That is, the ACFs and PACFs are flat.

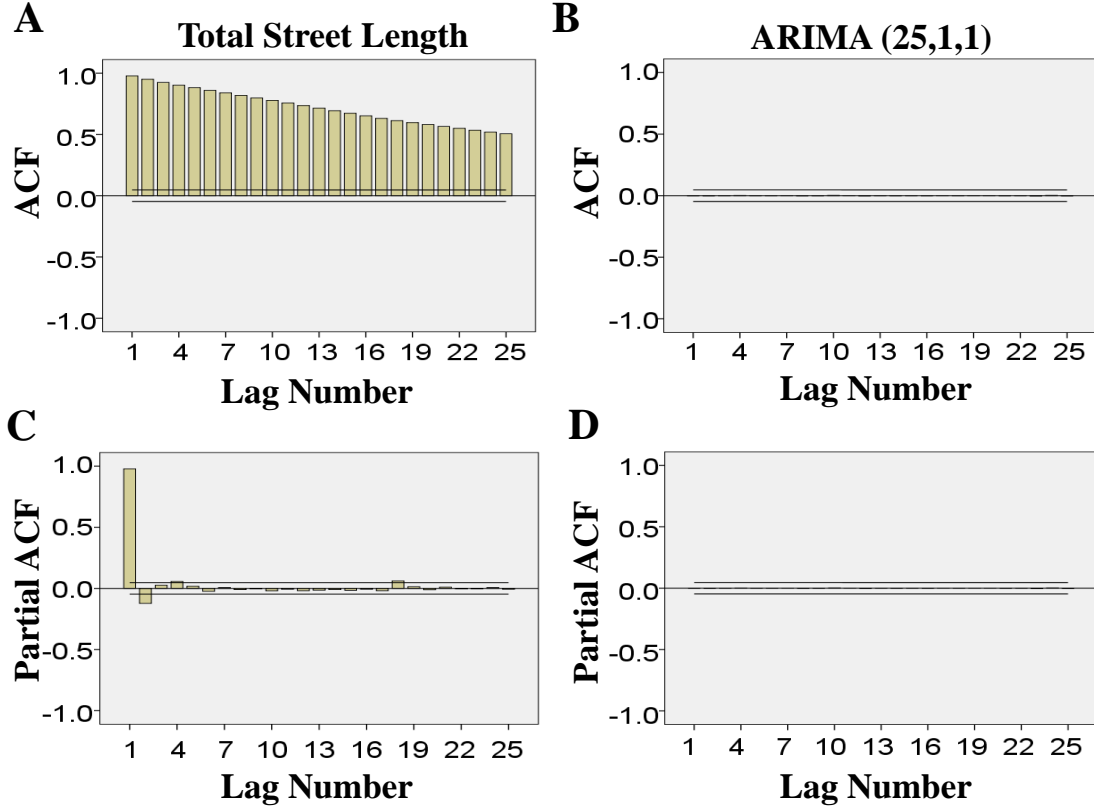


Figure 2.9: ACF structure of total street length from subject 2 before (A) and after (B) applying an ARIMA(25,1,1) model. PACF structure of total street length recorded from the same subject before (C) and after (D) applying the model. The black lines that are close to the reference zero-line, denote 95% statistical significance level from the ACF and PACF value. Notice that the strong autocorrelation and partial-autocorrelation structure on the raw data disappeared after applying ARIMA(25,1,1) modeling. That is, the ACFs and PACFs are flat.

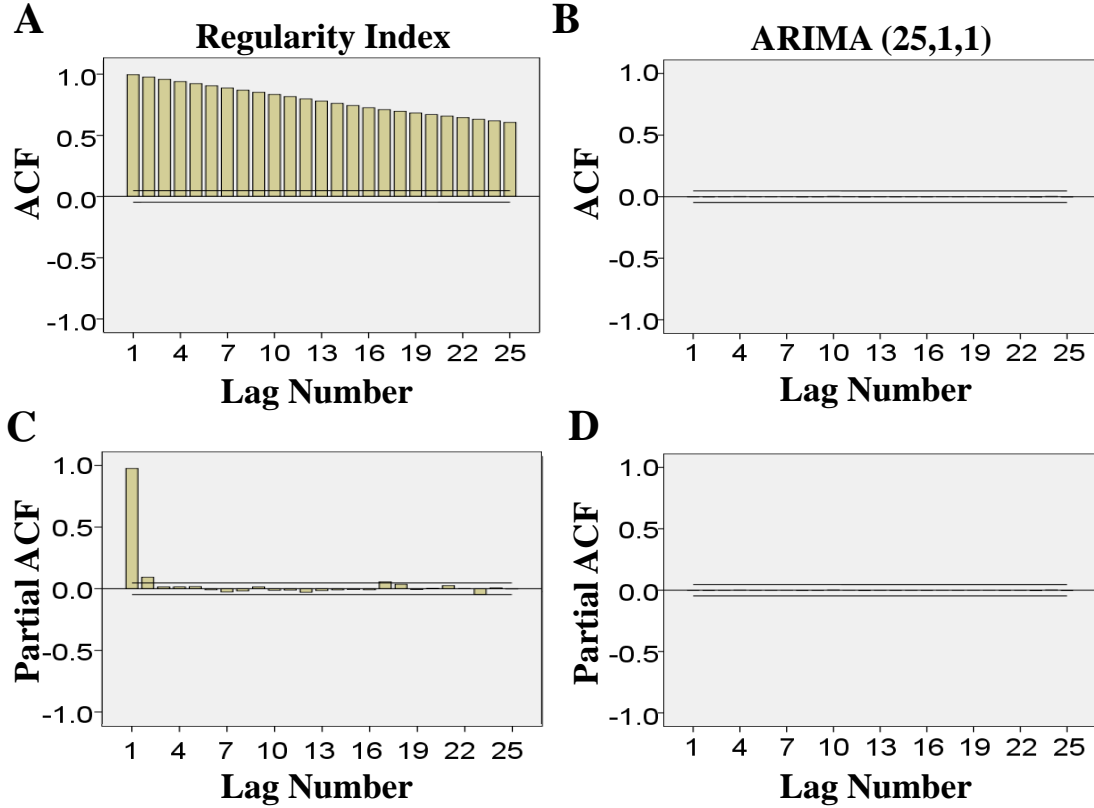


Figure 2.10: ACF structure of regularity index from subject 2 before (A) and after (B) applying an ARIMA(25,1,1) model. PACF structure of regularity index recorded from the same subject before (C) and after (D) applying the model. The black lines that are close to the reference zero-line, denote 95% statistical significance level from the ACF and PACF value. Notice that the strong autocorrelation and partial-autocorrelation structure on the raw data disappeared after applying ARIMA(25,1,1) modeling. That is, the ACFs and PACFs are flat.

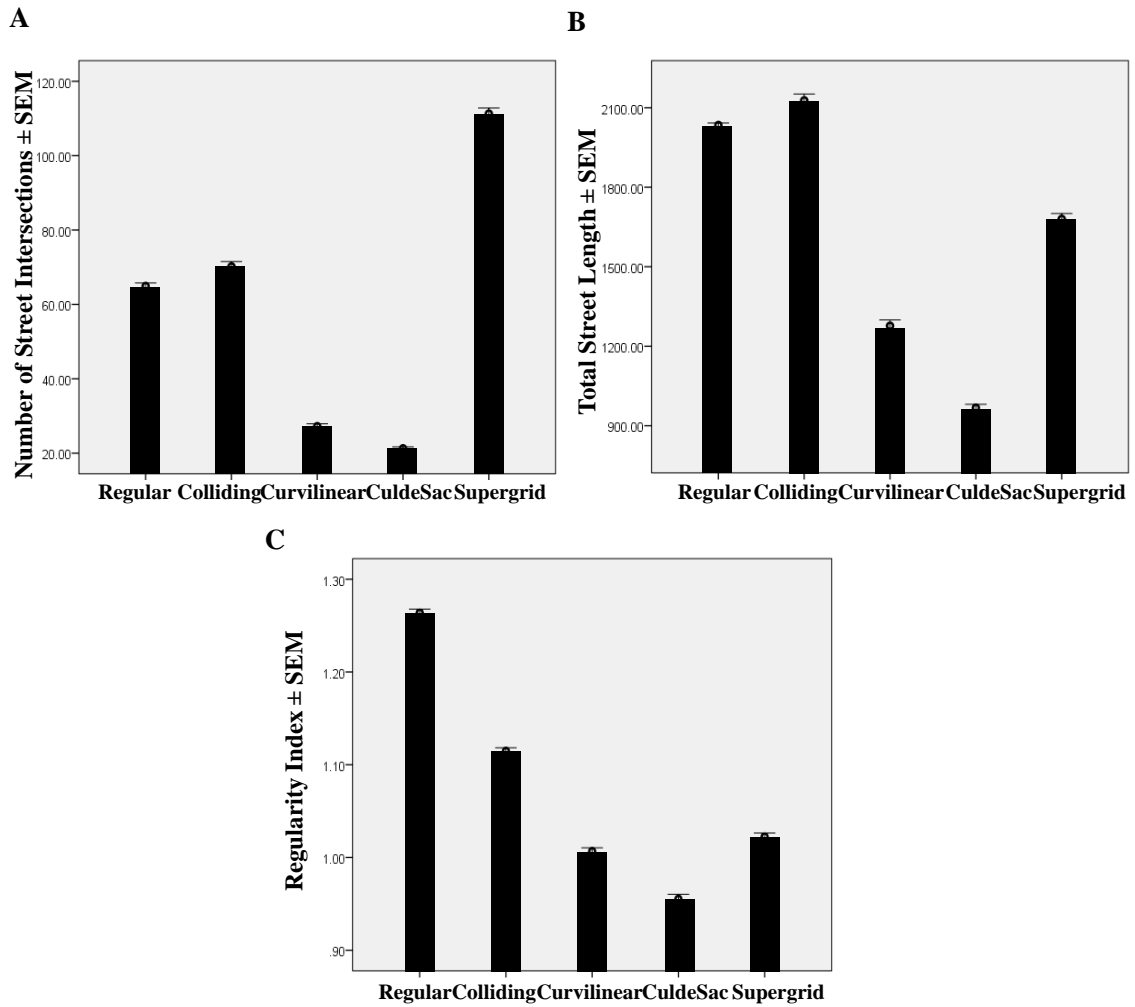


Figure 2.11: Mean \pm standard error of mean of (**A**) number of street intersections, (**B**) total street length, and (**C**) regularity index, across 10 subjects for each street network type.

Table 2.1: Number of cases, mean, and standard deviation of space syntax parameters across *regular grids* for each subject.

Grid Type	Subject		Street Intersections		Street Length		Regularity Index	
		N	Mean	Std	Mean	Std	Mean	Std
REGULAR	1	3529	62.719	8.0323	2003.896	138.871	1.268	.093
	2	405	67.643	13.702	2072.392	184.705	1.282	.127
	3	3068	63.689	11.388	2045.300	163.387	1.276	.116
	4	574	63.027	8.959	1990.181	148.074	1.249	.112
	5	329	67.082	12.349	2063.765	207.201	1.277	.127
	6	1112	60.247	6.574	2047.412	107.728	1.254	.099
	7	1053	69.111	12.332	2038.857	218.552	1.257	.139
	8	1376	65.750	11.792	2014.128	183.968	1.252	.123
	9	556	64.979	10.160	2035.217	169.695	1.272	.122
	10	1611	64.955	11.234	2031.708	196.494	1.251	.114

Table 2.2: Number of cases, mean, and standard deviation of space syntax parameters across *colliding grids* for each subject.

Grid Type	Subject		Street Intersections		Street Length		Regularity Index	
		N	Mean	Std	Mean	Std	Mean	Std
COLLIDING	1	3244	68.802	13.485	2129.262	232.844	1.133	.093
	2	320	68.546	13.132	2090.117	256.261	1.127	.080
	3	4755	72.591	13.354	2206.353	300.483	1.109	.063
	4	733	66.043	13.102	2084.185	276.157	1.094	.099
	5	375	67.318	14.367	2098.050	314.940	1.115	.088
	6	882	71.288	14.533	2187.589	292.055	1.107	.069
	7	547	69.256	13.326	2124.788	251.878	1.119	.090
	8	2323	66.804	14.840	2006.680	257.954	1.109	.081
	9	601	80.531	15.107	2271.397	228.231	1.123	.067
	10	1103	70.684	15.101	2076.574	287.122	1.112	.064

Table 2.3: Number of cases, mean, and standard deviation of space syntax parameters across *curvilinear grids* for each subject.

Grid Type	Subject		Street Intersections		Street Length		Regularity Index	
		N	Mean	Std	Mean	Std	Mean	Std
CURVILINEAR	1	3684	28.488	7.758	1323.816	282.092	.995	.059
	2	394	25.894	10.543	1245.036	380.768	1.003	.071
	3	3996	28.707	8.183	1338.457	290.385	1.001	.054
	4	639	30.245	8.199	1362.406	303.018	1.004	.058
	5	742	22.927	9.784	1132.481	310.476	1.037	.063
	6	925	27.233	7.162	1254.592	249.813	1.001	.065
	7	1291	29.082	8.088	1351.547	290.989	.998	.057
	8	1979	26.977	9.388	1275.021	338.893	1.015	.061
	9	971	27.368	8.327	1262.954	295.019	1.005	.064
	10	1706	25.317	9.434	1224.009	328.382	1.008	.070

Table 2.4: Number of cases, mean, and standard deviation of space syntax parameters across *cul-de-sacs* for each subject.

Grid Type	Subject		Street Intersections		Street Length		Regularity Index	
		N	Mean	Std	Mean	Std	Mean	Std
CUL-DE-SAC	1	3895	23.256	3.913	1027.046	119.783	.949	.083
	2	335	21.370	4.538	973.505	178.713	.950	.094
	3	4212	19.368	5.481	920.799	175.168	.951	.080
	4	670	20.769	5.132	939.319	169.042	.964	.072
	5	364	21.413	5.890	971.311	202.701	.934	.091
	6	942	21.602	3.919	985.758	124.965	.974	.077
	7	1722	20.987	5.663	944.522	183.276	.936	.082
	8	1279	23.494	3.013	1039.458	96.378	.949	.086
	9	1417	19.168	5.485	910.330	160.466	.984	.107
	10	2175	21.147	5.329	963.712	140.7432	.962	.087

Table 2.5: Number of cases, mean, and standard deviation of space syntax parameters across *supergrids* for each subject.

Grid Type	Subject		Street Intersections		Street Length		Regularity Index	
		N	Mean	Std	Mean	Std	Mean	Std
SUPERGRID	1	2723	111.219	26.814	1699.338	256.793	1.022	.058
	2	344	111.404	28.640	1673.370	254.444	1.025	.068
	3	3936	109.278	27.022	1709.996	261.988	1.027	.058
	4	773	99.932	22.453	1536.855	310.056	.995	.070
	5	576	111.057	30.959	1671.167	301.636	1.013	.076
	6	1682	111.866	29.199	1709.853	280.628	1.016	.071
	7	2097	111.737	34.195	1649.006	304.396	1.034	.073
	8	2423	113.648	33.424	1651.404	271.653	1.026	.062
	9	1717	119.988	25.876	1797.478	244.501	1.042	.062
	10	1483	112.744	27.044	1703.687	253.932	1.024	.057

2.4.3 Relation between neural activity and map parameters

To look at the relationship between the ongoing neural activity and space syntax parameters, we performed multivariate multiple linear regression analyses to regress the MEG time series on each of the space syntax parameters, Eq. (2.4)-(2.6). We then used the absolute t -values ($P < 0.05$) corresponding to the regression coefficients to get a measure of the significance of the relations.

Results revealed statistically significant relations between the ongoing neural activity and space syntax parameters. Fig. 2.12 illustrates the spatial distributions of the 248 MEG sensors involved in the processing of space syntax parameters. Red color indicates sensors highly associated with the processing of a space syntax parameter, whereas blue indicates sensors that are not involved in space syntax processing. Interestingly, there is a strong focus of space syntax sensors in the right frontal cortex, Fig. 2.12. Particularly, processing of total street length and regularity index involved predominantly right frontal and prefrontal areas, Fig. 2.12 (panels B and C). With respect to the regularity index, there is also a strong focus on cerebellum and right temporal cortex, Fig. 2.12 (panel C). Finally, processing of street network type revealed patches mainly in prefrontal areas, Fig. 2.12 (panel A).

These findings raised the question of whether the neural processing of space syntax parameters differs between street network layouts. To address this question, we performed for each grid the same regression analysis, Eq. (2.4)-(2.6). Figures 2.13-2.15 illustrate the spatial distributions of the sensors involved in the processing of number

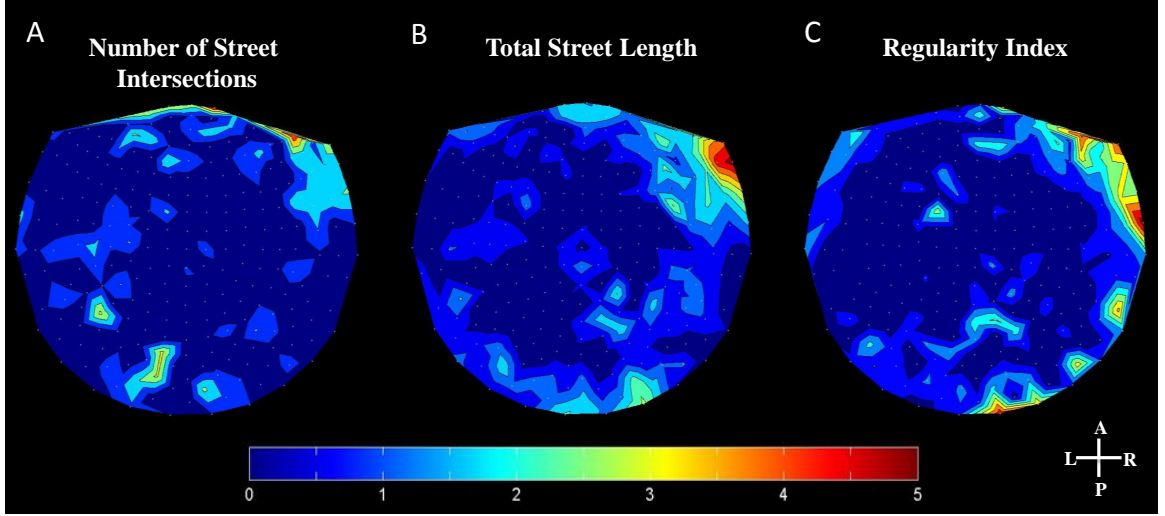


Figure 2.12: Spatial distributions of the neural processing of (A) number of street intersections, (B) total street length, and (C) regularity index, across all street network types. 2-D contour plots in the MEG sensor space of the mean absolute t -values ($P < 0.05$) across 10 subjects corresponding to the regression coefficients of space syntax parameters in the linear regressions, Eq. (2.4)-(2.6).

of street intersections, total street length, and regularity index respectively, for each street network type. There are several interesting findings. Overall, processing of number of street intersections and total street length involved mainly right frontal and prefrontal areas for regular, colliding, and curvilinear street network layouts, Fig. 2.13-2.15 (panels A, B, and C). However, cul-de-sacs and supergrids involved minimal processing of these space syntax characteristics, Fig. 2.13-2.15 (panels D and E) .

Particularly, with respect to the number of street intersections, Fig. 2.13, there is a strong focus on orbitofrontal areas (OFC) for regular (panel A) and colliding grids (panel B), and on bilateral prefrontal, right frontal-temporal and cerebellar areas for curvilinear grids (panel C). Processing of total street length for regular

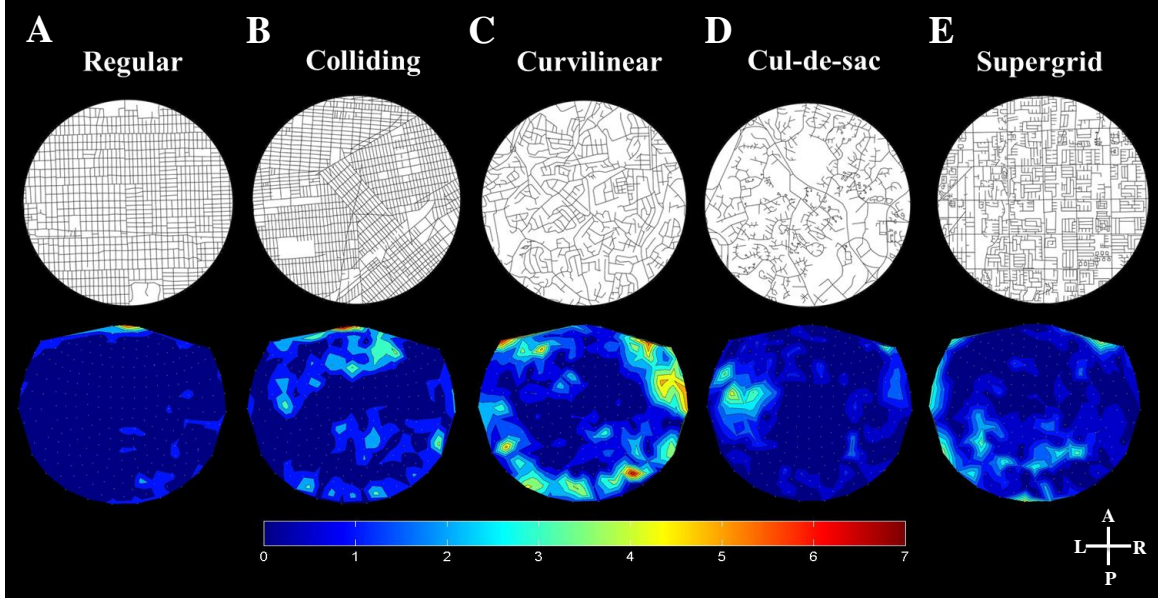


Figure 2.13: Spatial distributions of the neural processing of *number of street intersections* for each street network type. First row illustrates example stimuli from (A) regular, (B) colliding, (C) curvilinear, (D) cul-de-sac, and (E) supergrid street network layouts. Second row illustrates 2-D contour plots in the MEG sensor space of the mean absolute t -values across 10 subjects ($P < 0.05$) corresponding to the regression coefficients of number of street intersections in the linear regressions for each street network type respectively, Eq. (2.4).

street networks mainly involved right prefrontal, cerebellar, and parieto-occipital cortex, Fig. 2.14 (panel A). For colliding grids, total street length sensors were focused mainly on right prefrontal and secondarily on right frontal cortex, Fig. 2.14 (panel B), whereas for curvilinear grids they were localized on right prefrontal and cerebellar areas, Fig. 2.14 (panel C). Finally, with respect to the regularity index, Fig. 2.15, there is a strong focus on right prefrontal and parieto-occipital areas for regular grids (panel A). Colliding street networks involved minimal processing of regularity index, associated with prefrontal areas (panel B). For cul-de-sacs (panel D), supergrids (panel E), and curvilinear grids (panel C) the association of regularity index with neural signal

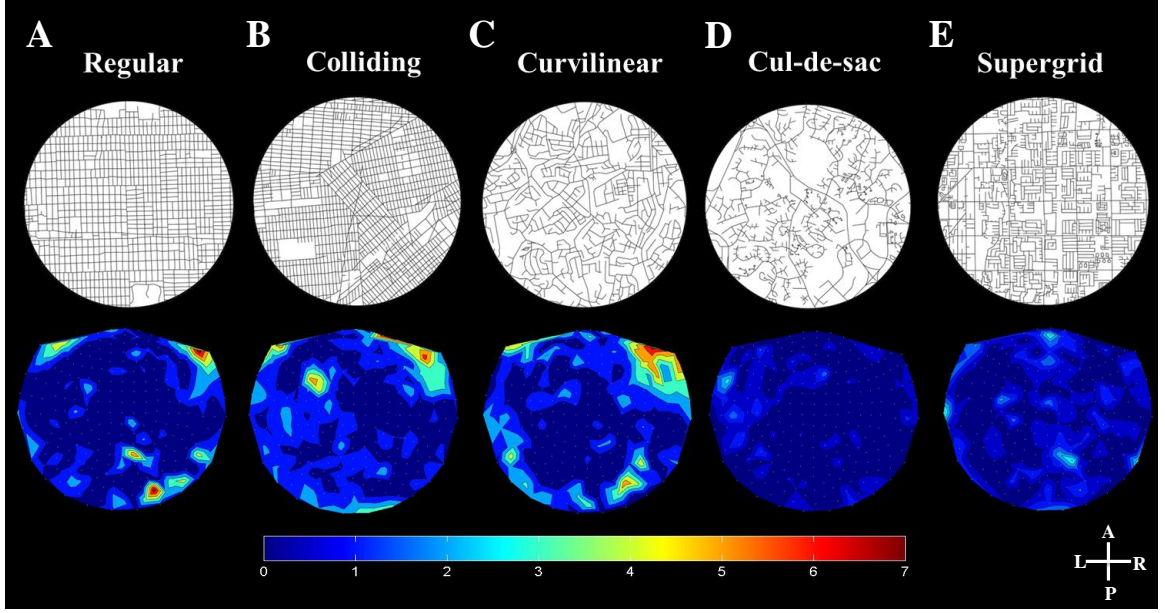


Figure 2.14: Spatial distributions of the neural processing of *total street length* for each street network type. First row illustrates example stimuli from (A) regular, (B) colliding, (C) curvilinear, (D) cul-de-sac, and (E) supergrid street network layouts. Second row illustrates 2-D contour plots in the MEG sensor space of the mean absolute t -values across 10 subjects ($P < 0.05$) corresponding to the regression coefficients of total street length in the linear regressions for each street network type respectively, Eq. (2.5).

was minimal.

We then used hierarchical cluster analysis to map changes in the neural processing of a space syntax parameter for different types of street networks. This method clusters the spatial distributions of the sensors involved in the processing of a space syntax parameter for each street network type, according to a similarity measure. Similarity of the neural processing of a space syntax parameter between two grids was assessed by computing the RMS value of the difference between the absolute t -values corresponding to this space syntax parameter of the two grids, Eq. (2.7) (see section 2.3). Street network types included in the same cluster, then, can be judged to involve

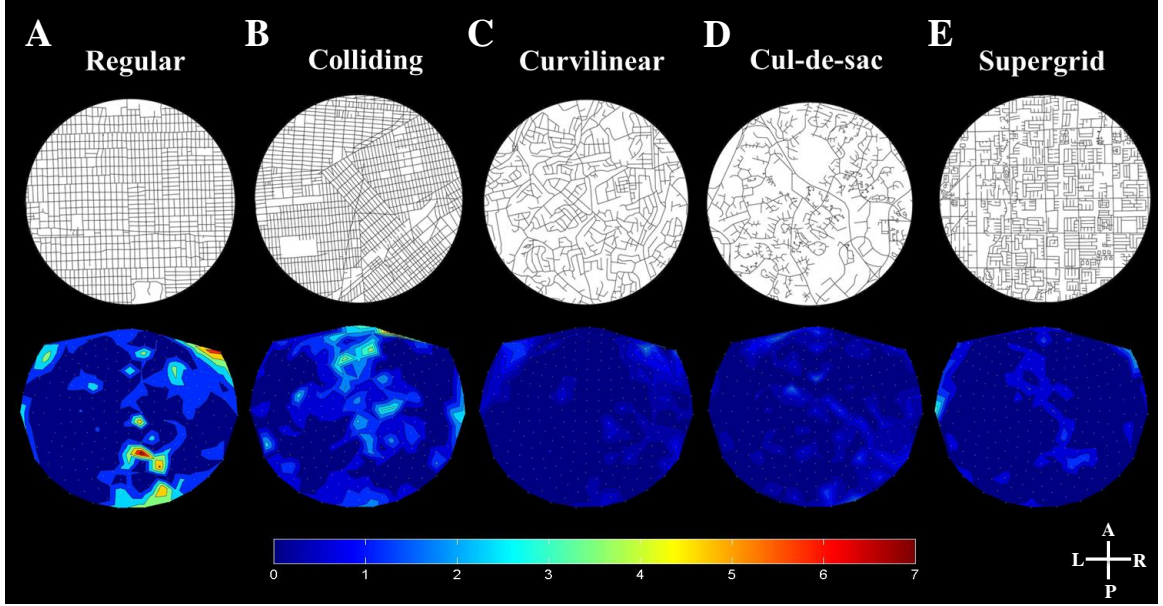


Figure 2.15: Spatial distributions of the neural processing of *regularity index* for each street network type. First row illustrates example stimuli from (A) regular, (B) colliding, (C) curvilinear, (D) cul-de-sac, and (E) supergrid street network layouts. Second row illustrates 2-D contour plots in the MEG sensor space of the mean absolute t -values across 10 subjects ($P < 0.05$) corresponding to the regression coefficients of regularity index in the linear regressions for each street network type respectively, Eq. (2.6).

similar neural processing of a space syntax parameter. The results of hierarchical tree clustering are summarized by dendrograms, which indicate at what level of similarity any two clusters were joined. With respect to the number of street intersections, Fig. 2.16, cul-de-sac and supergrid are the most similar, and join to form the first cluster. Note that they were both minimally involved in the neural processing of number of street intersections, Fig. 2.13 (panels D and E). Then, regular grid joined to form the second cluster, followed by the joining of colliding grid at distance 6. Finally, curvilinear grid merged at distance 25, indicating neural processing that differs from the other street network types. This is true, since the sensors associated

with number of street intersections for curvilinear grids were more widely distributed than the ones for the rest street network layouts, Fig. 2.13 (panel C). Similarly, with respect to the total street length, Fig. 2.17, cul-de-sac and supergrid merged at close distance to form the first cluster, followed by the joining of curvilinear grid, at distance 9. Colliding grid joined at distance 14, and regular grid merged at distance 25. Long distances between clusters indicate the dissimilarity in the neural processing of total street length between different street network types. Finally, for the neural processing of regularity index, Fig. 2.18, curvilinear, cul-de-sac, and supergrid merged in the same cluster at distance 3, since they involve minimal processing of this parameter, Fig. 2.15 (panels C, D, and E). Colliding grid joined at distance 15, followed by regular at distance 25. Note that neural processing of regularity index was involved mainly in regular and secondarily in colliding grid, Fig. 2.15 (panels A and B).

2.5 Discussion

In recent years, scientists have made significant progress in understanding the neural basis of decision-making. The vast majority of these studies have heavily focused on economic decisions, in which the main question is how the brain computes, represents and compares values of alternative items/goods to select the best alternative. According to these studies, the brain integrates all the decision variables related with an option (e.g., price, quality, brand, etc) into a single value that characterizes the subjective value of this option [48,50,51]. Decision is made after comparing the subjective

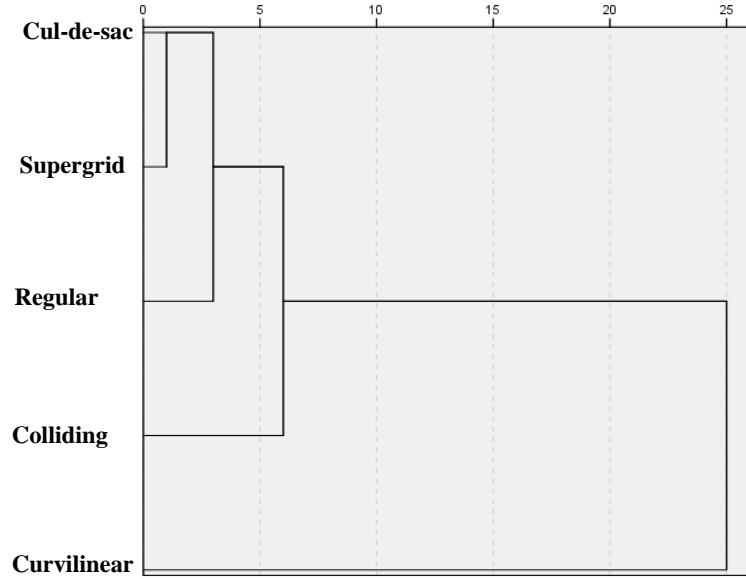


Figure 2.16: Dendrogram (using the average linkage between groups) displaying the clusters resulting by joining the grids that are most similar, in terms of their spatial distributions in the MEG sensor space of the absolute t -values corresponding to the number of street intersections.

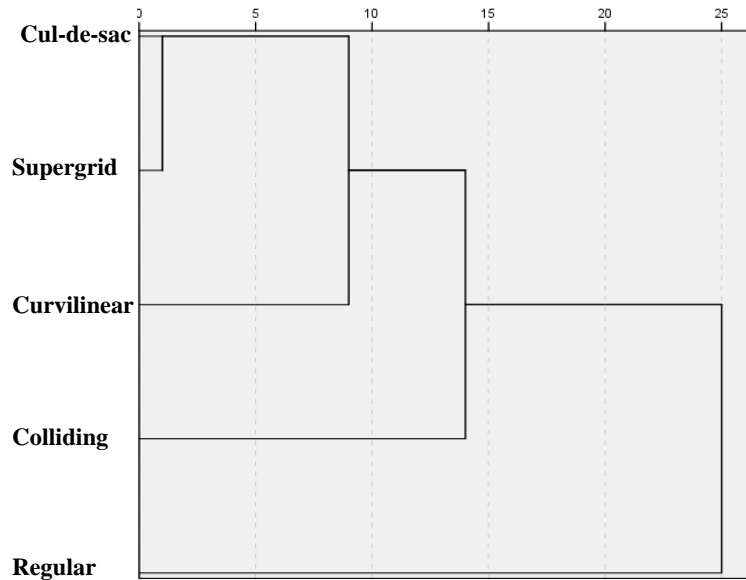


Figure 2.17: Dendrogram (using the average linkage between groups) displaying the clusters resulting by joining the grids that are most similar, in terms of their spatial distributions in the MEG sensor space of the absolute t -values corresponding to the number of total street length.

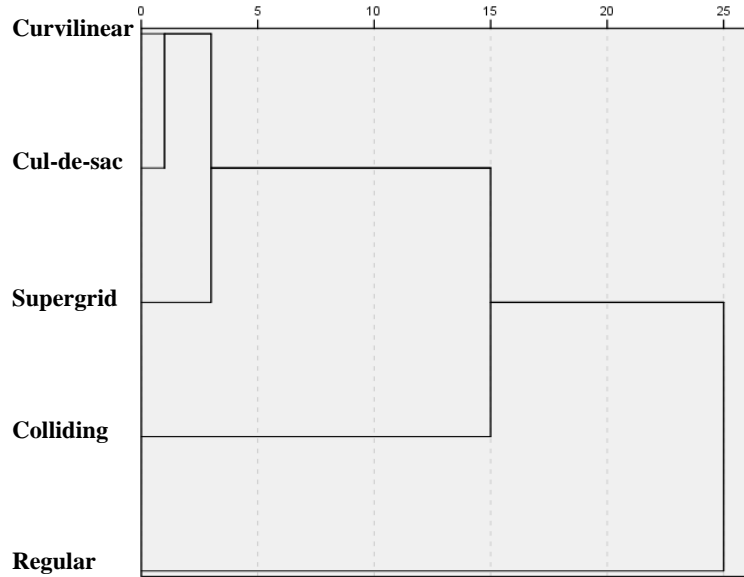


Figure 2.18: Dendrogram (using the average linkage between groups) displaying the clusters resulting by joining the grids that are most similar, in terms of their spatial distributions in the MEG sensor space of the t -absolute values corresponding to the regularity index.

values of available options to find the best alternative. The main characteristic in economic choices is that subjective values depend on the options themselves. While economic choice is an important component of human behavior, people frequently have to select between options whose values are strongly dependent on the spatial characteristics of the environment. It is also likely that the values are not immediately evident before exploring and/or navigating within the environment where the alternatives are located. For instance, when looking for a new house, the values of the alternative options depend also on the spatial characteristics of the areas that houses are located, such as distance from work, accessibility to highways, etc. Evaluating these characteristics may involve map exploration and/or navigation around these areas. How the brain represents and processes spatial information acquired during

exploration to make decisions is still poorly understood.

In the current study, we conducted a novel brain imaging experiment to test the hypothesis that a network of cortical regions is involved in the processing of spatial information acquired during exploration to a make decision. We recruited 10 subjects and asked them to explore small city maps, exemplifying five different street network types (i.e., regular, colliding, curvilinear, cul-de-sac, and supergrid) to build a hypothetical City Hall, while neuronal activity was recorded continuously by 248 MEG sensors at high temporal resolution. We also monitored subjects' eye positions to locally characterize the maps by computing three space syntax parameters within the circular areas of 6 DVA radius centered on each eye position ("eye's mind"): a) total street length, b) number of street intersections, and c) regularity index. After preprocessing both MEG time series and space syntax parameters time series to render stationary data, we performed a linear regression analysis for each street network layout to regress the time-varying MEG signal from the 248 sensors on each of the space syntax parameters.

In line with our initial hypothesis, we found that ongoing neural activity was strongly associated with space syntax parameters through localized and distributed networks. Interestingly, right frontal and prefrontal areas were predominantly involved in the processing of all space syntax parameters. Even though this finding is somehow counter-intuitive since higher cognitive brain regions have long been associated with the evaluation/comparison of values in economic choices [44], recent studies in rodents suggest that frontal areas encode also spatial variables needed to define

specific behavioral goals in navigation and way-finding tasks [23]. Another possible scenario is that these parameters were used for the evaluation of different locations in the map. It is likely that during map exploration, subjects used these (and possible other) parameters to evaluate and compare the “attractiveness” of the locations they were exploring. In that way, space syntax parameters can be considered as decision variables that characterize the values of alternative locations, and therefore, are encoded in the frontal areas of the brain.

Additionally, neural processing of the regularity index also involved right temporal and cerebellar areas. It has been suggested that temporal areas, such as inferior temporal cortex (IT), encode the position of different objects presented in a scene [1]. The regularity index in a broad sense characterizes the relative positions between the street intersections (i.e., it measures the degree to which the distribution of street intersections deviates from complete spatial randomness to either clustering or regularity), and so, it may be encoded by IT. The cerebellum has long been exclusively associated with motor control and high cognitive functions, such as attention [81]. However, recent studies provide evidence that it also participates in spatial information processing. In particular, behavioral and neurophysiological studies in cerebellar mutant mice showed that the cerebellum interacts and communicates with the hippocampus to participate in the construction of the “cognitive map” (for review see [65]). In terms of the anatomical connection between these two regions, although a direct cerebello-hippocampal projection has been suggested, recent findings argue against this theory suggesting a multi-synaptic pathway involving posterior parietal

cortex and retrosplenial cortices [61, 65].

It is important to point out that the associations between neural activity and space syntax parameters do not reflect eye movements, since x - y eye positions were used as covariates in the regression analyses. Additionally, these associations are not due to the locations of the receptive visual fields mapped outside the space syntax context of map exploration, in that receptive field centers and space syntax characteristics were not spatially distinguishable.

Our findings raised the question of whether the processing of space syntax parameters differs among the 5 street network types. To address this question we performed the same regression analyses, but now for each street network type. Results showed that neural processing of the number of street intersections and total street length mainly involved frontal and pre-frontal areas, but only for regular, colliding, and curvilinear grids. Instead, cul-de-sacs and supergrids involved minimal processing of these two space syntax parameters. These findings suggest that the number of street intersections and total street length are important spatial features for deciding among many options where to build the hypothetical City Hall, but only for regular, colliding, and curvilinear street network types. On the contrary, people seem to ignore these parameters when exploring cul-de-sacs and supergrids, suggesting that they may use other kinds of information to make a decision. Regarding the regularity index, there was a strong focus on right prefrontal and parieto-occipital areas for regular grids, and a weaker focus on prefrontal cortex for colliding grids. On the other hand, there was minimal or no processing of the regularity index for cul-de-sacs, supergrids, and

curvilinear grids. Based on these findings, regularity index seems to be an important spatial characteristic for the evaluation of the alternative locations to find the best place for the hypothetical City Hall, but only for regular and colliding grids. This is also inline with the fact that the regularity index is significantly higher for regular and colliding grids compared to the rest of the street network types.

Overall, we presented a novel brain imaging study to assess the relation between neural activity and particular space syntax parameters. The results complement behavioral findings from a series of previous studies, suggesting that people use spatial characteristics of the environment to make decisions. To the best of our knowledge, this is the first study showing that spatial information required to make decisions is encoded through localized and distributed brain areas. These results suggest new avenues to elucidate the neural basis of spatial information processing in exploration and decision-making.

Chapter 3

Cognitive mechanisms underlying instructed choice exploration of small city maps

3.1 Overview

To make good decisions within a novel environment people have to explore the environment. Exploration is considered the process through which we learn the structure of the environment so that we understand the consequences of our decisions. But how people explore novel environments to make decisions is still poorly understood. The purpose of this study is to understand the cognitive mechanisms underlying exploration and decision making in realistic and novel environments. We present an instructed choice experiment in which subjects explored small maps of U.S. cities ex-

emplifying five different types of street networks, in order to place a hypothetical Post Office at one of two possible locations. Monitoring eye positions revealed restricted map exploration determined by the position of the two alternative options and the center of the stimulus. Subjects were continuously exploring the areas around the two options and the center of the map by repeatedly looking back and forth between them before deciding which one to choose, presumably implementing a comparison process. Selection of an option was highly associated with the time spending exploring the area around that option, with subjects spending more time exploring the area around the option they finally selected. Finally, results suggest that first and last fixation sets have an important role in influencing the value of the alternative options, and thus, biasing the decision. Overall, the initial fixations around an option favored the location ultimately chosen. These results suggest that human strategies are highly stereotyped in exploring novel environments for making spatial decisions, and these strategies share many common characteristics with the way that humans make economic choices.

3.2 Introduction

Consider a hypothetical scenario that you have been accepted by a graduate school and you were visiting the university for the first time to find a house to rent. The school provides you with a map that marks the student houses around campus and also gives you information about the bus stations, classrooms, libraries, food service,

etc. Abstractly, you face an example of a common decision problem, in which you have to explore and evaluate all the alternative options to find the best place to rent. Choosing between alternative options requires assigning and integrating values along a multitude of dimensions (e.g., rental rate, amenities, distance from school, etc.). How do people explore novel environments to extract information and make decisions is considered one of the fundamental problems in decision neuroscience. After many years of intense research in disciplines ranging from psychology to economics, we have made significant progress in understanding the cognitive mechanisms of decision-making in a variety of tasks. A series of experimental studies in both humans and animals provide compelling evidence that the brain makes simple decisions by integrating all the decision determinants of an option into a subjective value, and then it compares these values to make a choice [48, 50, 51, 62, 66, 82]. Although these studies have contributed significantly to understanding the cognitive mechanisms of decision making, they have heavily focused on simple decisions that take place in artificial environments, and most importantly, the values of the alternative options depend only on the options themselves and not on the environmental properties.

While in many decisions the environmental properties do not influence the economic values of the alternatives, such as deciding between products in a grocery store, there are other cases in which the value of an option strongly depends on its environment. For instance, student houses that are closer to campus are usually more expensive than distant houses, even when they share similar characteristics. Solving this type of decision problem, like any other executive process, requires exploring the

surroundings of the alternative options, extracting information about the properties of the environment, and integrating this information with value information related to the options themselves.

In the current study, we designed a novel psychophysical experiment to investigate how people explore realistic environments to make decisions. We used a set of real maps of various U.S. metropolitan cities with different street network types, and marked two locations. We recruited 12 subjects and asked them to explore the maps and select one of the two locations to build a hypothetical Post Office. We found that human strategies in map exploration for decision making share many characteristics with the strategies that people adopted in economic choices problems. Particularly, monitoring eye positions revealed that subjects were spending more time exploring the area around the option they finally selected than the option that was not selected at the end of the trial. This finding has also been reported in many value-based decision studies [35,36,59,69,70,80] suggesting that eye fixation guides the comparison process and modulates the value assigned to fixated location.

We also found that subjects were continuously exploring the areas around the two alternative options and the centers of the maps before making their decision, by looking back and forth between them. This kind of behavior has also been found in many decisions between multiple items, in which people were looking repeatedly at them, presumably implementing a comparison process between the subjective values of the items [35, 36, 80]. However, in all these studies, subjects did not fixate at any other location besides around the items. This is an important difference with

our study, in which people spent a significant amount of time fixating at the area around the center of the map, even when the two alternative options were in close distance. Finally, a key finding was that subjects showed a strong bias to select the option that they firstly explored. This behavior has also been reported in value-based decisions [35], suggesting that the first fixation may have an important role in influencing the value of the alternative options, and thus, biasing the decision. All these findings suggest that humans adopted highly stereotype strategies to explore novel environments and make spatial decisions. These strategies share many common characteristics with the strategies that people followed to make decisions between options that have economic consequences.

3.3 Materials and methods

3.3.1 Subjects

Twelve healthy right-handed subjects, 6 women and 6 men, participated in this study for monetary compensation. They ranged in age from 19 to 58 years (women's age 36.8 ± 5.8 years, mean \pm SEM; men's age 38.8 ± 7 years). The age did not differ significantly between the two genders ($P = 0.36$, t-test). The appropriate Institutional Review Board approved the study protocol, and an informed consent was obtained from all the participants based on the Declaration of Helsinki.

3.3.2 Stimuli

The stimuli were circular maps of 1-mile diameter urban areas extracted from street center-line maps, representing several U.S. Metropolitan Statistical Areas (Atlanta, GA; Baltimore, MD; Chicago, IL; Los Angeles, CA; New York, NY; Pittsburgh, PA; St. Louis, MO; Tampa, FL; Washington, DC). The choice of the stimuli was based on studying how subjects respond to the spatial structure of the street network, and particularly its shape, density and connectivity.

The sample was chosen to exemplify five different street networks types, namely: (i) *regular grids*, i.e., orthogonally intersecting patterns of streets, (ii) *colliding grids*, i.e., multiple intersecting regular grids rotated with respect to one another, (iii) *curvilinear grids*, i.e., intersecting patterns of curvilinear streets, (iv) *cul-de-sacs*, i.e., hierarchically branching street networks, and (v) *supergrids*, i.e., sparsely spaced orthogonally intersecting main arteries with irregular street patterns filling-in the large blocks surrounded by the arteries. For more information on stimuli and how were selected see [10].

The stimuli had two targets presented on the periphery of each map display, Fig. 3.1. The positions of the two targets were selected randomly, under the constraint of not being at an empty space. Four stimuli per street network type (totally 20) were presented to each subject in a pseudorandom sequence.

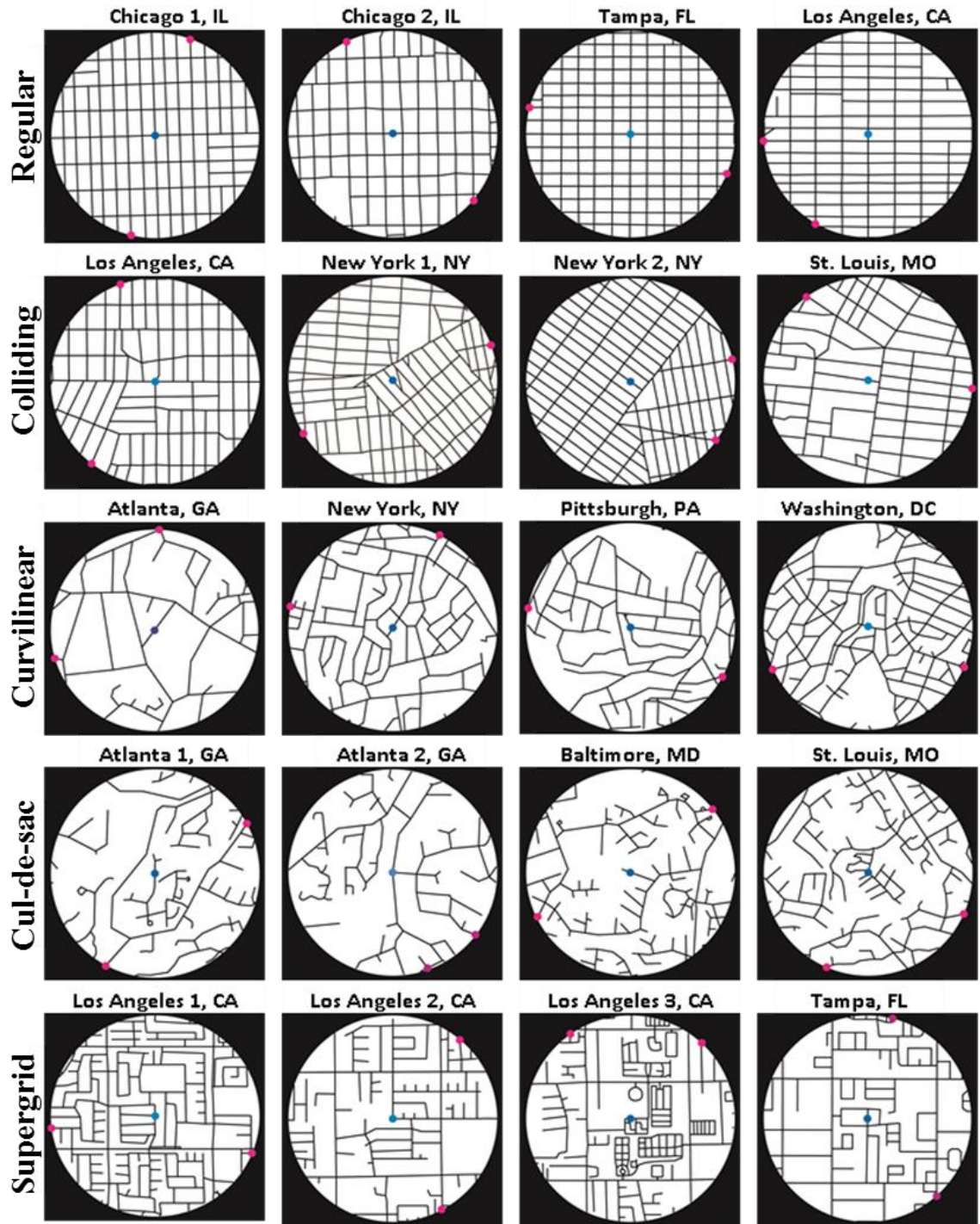


Figure 3.1: Map stimuli. Magenta dots denote the two potential locations (targets) for the Post Office. Blue dot marks the center of the map (shown here for illustration purposes).

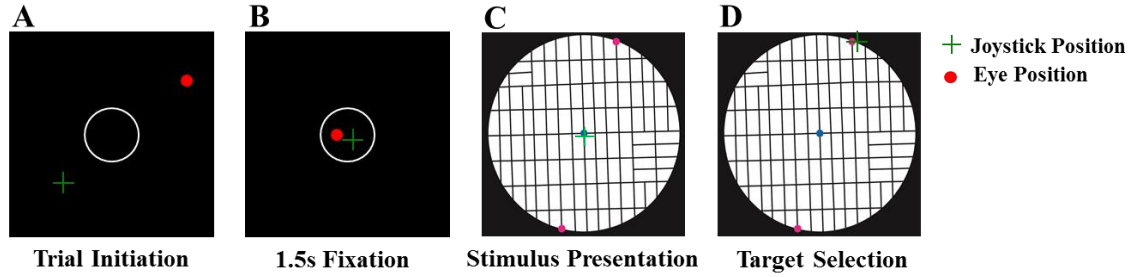


Figure 3.2: Task sequence. (A) Trial starts with the presentation of an open circle on the center of a black screen. (B) The subject is required to fixate eyes and place the mouse inside the circle for 1.5 s. (C) The stimulus is presented and subject explores the map by moving his/her eyes in order to decide between two alternative positions to place a hypothetical Post Office. (D) Subject chooses the Post Office location by clicking the mouse at the desired position.

3.3.3 Experimental Paradigm

Task

We developed an instructed choice exploration task that required subjects to explore small city maps in order to place a hypothetical post office at one of two possible locations, Fig. 3.2. At the beginning of the trial, an open circle was presented at the center of a black screen. Subjects were instructed to fixate their eyes and place the mouse inside that circle. After 1.5 s of fixating and holding at the center, the circle turned off and the stimulus appeared. Subjects were asked to choose between two alternative positions to place a hypothetical Post Office by clicking the mouse in the desired position. Subjects were instructed not to trace the path with the mouse cursor, and the experiment proceeded at their pace.

Experimental Set-up

Subject sat comfortably on a chair with chin and arm supported to stabilize the head and body. Subject's right forearm manipulating the mouse lay on a firm horizontal support. Stimuli were presented on a computer screen placed at eye level and at a distance of ~ 78 cm in front of the subject.

Data acquisition

The experiment was controlled by a program written in Visual basic (Microsoft Visual Basic 2005, version 8.0). Relevant data include the times of presentation of stimuli, the x - y position of the mouse (sampled at 200 Hz), and the x - y position of the eyes (sampled at 200 Hz). The eye position was recorded using a nonmagnetic video-based pupil/corneal reflection tracing system (model EGL-400, ISCAN, Inc. Burlington, MA).

Spatial analysis of eye positions

Isolines were used to characterize the overall spatial distribution of eye positions during map exploration. For each map, we superimposed the eye positions of all subjects and computed the probability density of eye positions. These probabilities were calculated as the ratio of the frequency that eye positions fell within a square ($67m \times 67m$) of a regular grid fitted to the map, to the total number of eye positions on the map. An isoline connects points in which the probability of the eyes exploring these points is the same. The value difference between any two consecutive isolines

is the contour interval, and values inside an isoline are higher than those outside. The colors of the isolines describe different levels of the contour intervals, with red corresponding to high probability density values and blue to low density regions.

We were interested to quantify the spatial patterns of the eye positions during map exploration, and particularly, how much of the exploration was attributed to the areas around the two targets and the center of the stimulus. We calculated across trials the mean density of eye positions (i.e., the mean percentage of eye positions) around the targets and the center of the stimulus, particularly, within the circular areas of 2, 4, 6, and 8 degrees of visual angle (DVA) radius centered on these locations. Fig. 3.3 displays an example of a single trial, illustrating the eye positions of a subject, and the circular areas of 2, 4, 6, and 8 DVA radius centered on the two targets and the center of the map.

To better assess whether the eye positions were more densely distributed around the selected targets versus the non-selected ones, and hence, to test the hypothesis that subjects spent more time exploring the chosen targets, we computed across trials the mean relative density of eye positions around the selected and non-selected targets. Mean relative density was computed as the ratio of the frequencies of eye positions within 4 DVA radius circles centered on the selected and non-selected targets, to the sum of the number of eye positions within these two circular areas (i.e., around the chosen and non-chosen targets).

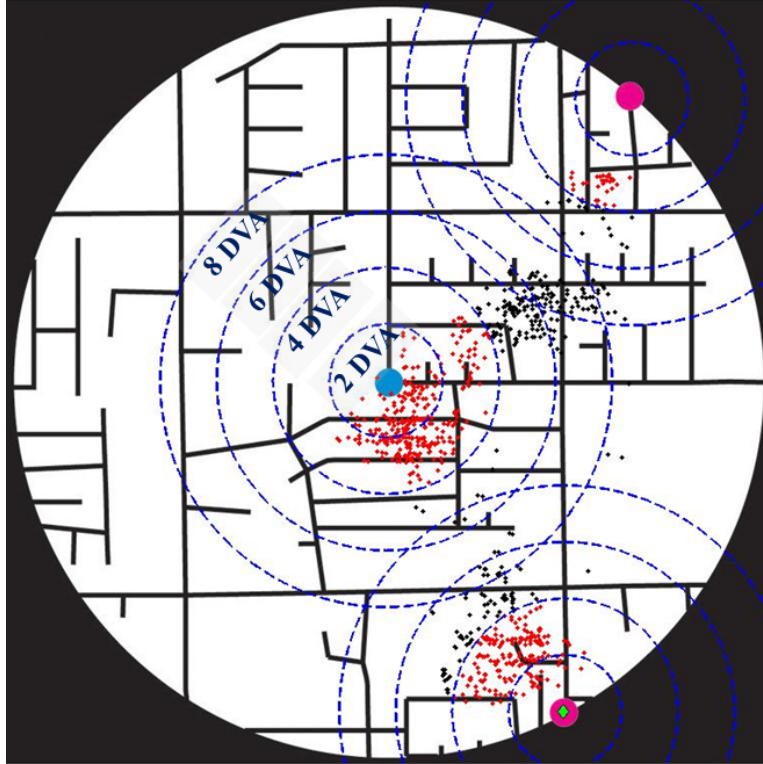


Figure 3.3: A single trial illustrating the eye positions (black and red dots) of a subject. Magenta dots mark the two targets, blue dot denotes the center of the map, and green diamond marks the selected target. Blue circles correspond to the circular areas of 2, 4, 6 and 8 degrees of visual angle radius centered on the two targets and the center of the map, and red dots are the eye positions within the areas of 4 DVA radius.

Temporal analysis of eye positions

To study the temporal evolution of the decision process, we computed the natural logarithmic ratio of the Euclidean distance between the instantaneous eye positions $(eye_{x,t}, eye_{y,t})$ at time t and the selected target $(Choice_x, Choice_y)$, to their Euclidean distance to the non-selected target $(NOTChoice_x, NOTChoice_y)$, Eq. (3.1).

$$\text{LogRatioDistance}_t = \ln \frac{\sqrt{(eye_{x,t} - Choice_x)^2 + (eye_{y,t} - Choice_y)^2}}{\sqrt{(eye_{x,t} - NOTChoice_x)^2 + (eye_{y,t} - NOTChoice_y)^2}} \quad (3.1)$$

This measure provides a metric of the eye trajectories, in terms of how close is the area that the eyes explore at time t to the selected target with respect to the non-selected one, with values less than zero corresponding to eye positions closer to the selected target, and vice-versa.

Statistical analysis

Data were analyzed using standard statistical methods and either the SPSS IBM statistical Package (version 21) or MATLAB (version R2013b).

3.4 Results

3.4.1 Decision Time

Subjects decided on the post office location after 4.113 ± 0.225 s (mean \pm SEM, $N = 236$ valid trials). Street network type did not affect the decision time ($F_{4,236} = 0.782$,

$P = 0.538$, partial $\eta^2 = 0.013$), nor did the target configuration (i.e., angle formed by the two radii of the targets) ($F_{19,236} = 0.823$, $P = 0.678$, partial $\eta^2 = 0.068$).

3.4.2 Spatial characteristics of eye positions

A previous study conducted in our lab showed that a free choice decision task, in which subjects were free to place a landmark at any feasible location, involves wide map exploration [10]. Here, we were interested in examining whether and how the elimination of the available options to only two potential locations affects the exploration of the city maps. Fig. 3.4 depicts the superimposed eye positions of all subjects on each map and the corresponding contour plots that describe the probability density of the eye positions by isolines (see Materials and methods section for more details). As revealed, people restricted the exploration space around the two alternative locations and the centers of the stimuli (see the contour intervals within the red isolines in Fig. 3.4). This pattern of eye positions was consistent across all maps irrespective of street network type and target configuration, suggesting that people adopted a specific strategy to explore maps for extracting the environmental information that will be used to make a decision.

To further quantify the spatial pattern of eye positions and, particularly, to study how much each of the targets and the center of the stimulus were involved in map exploration, we calculated the mean density across trials of the eye positions, within a circular area of 2, 4, 6, and 8 DVA centered on the selected target, the non-selected

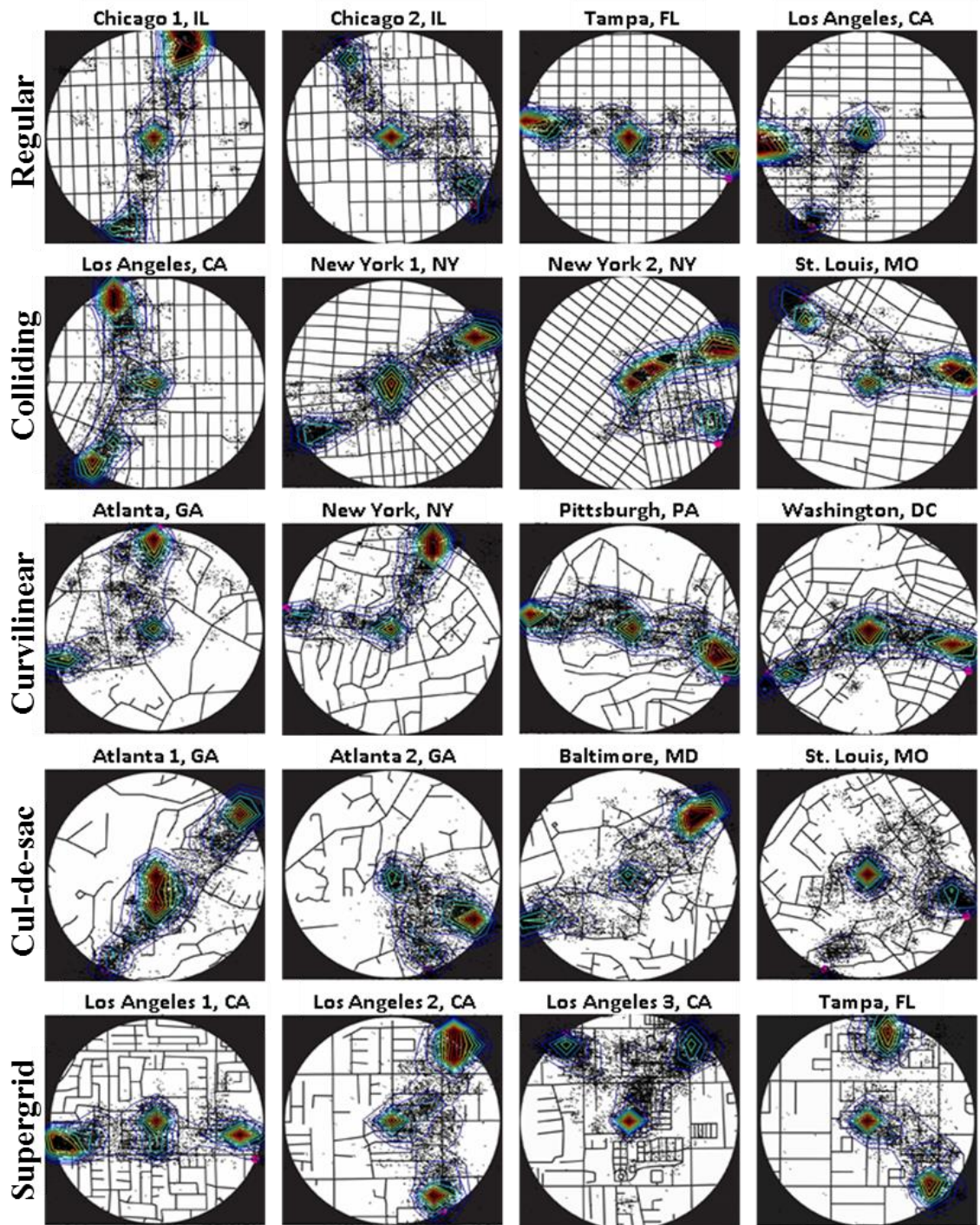


Figure 3.4: Superimposed eye positions (black dots) on each map of all 12 subjects, and the corresponding isolines illustrating the probability density of the eye positions. Isoline colors describe different levels (0 to 1) of the contour intervals, with red corresponding to high probability density values, and blue corresponding to low density values.

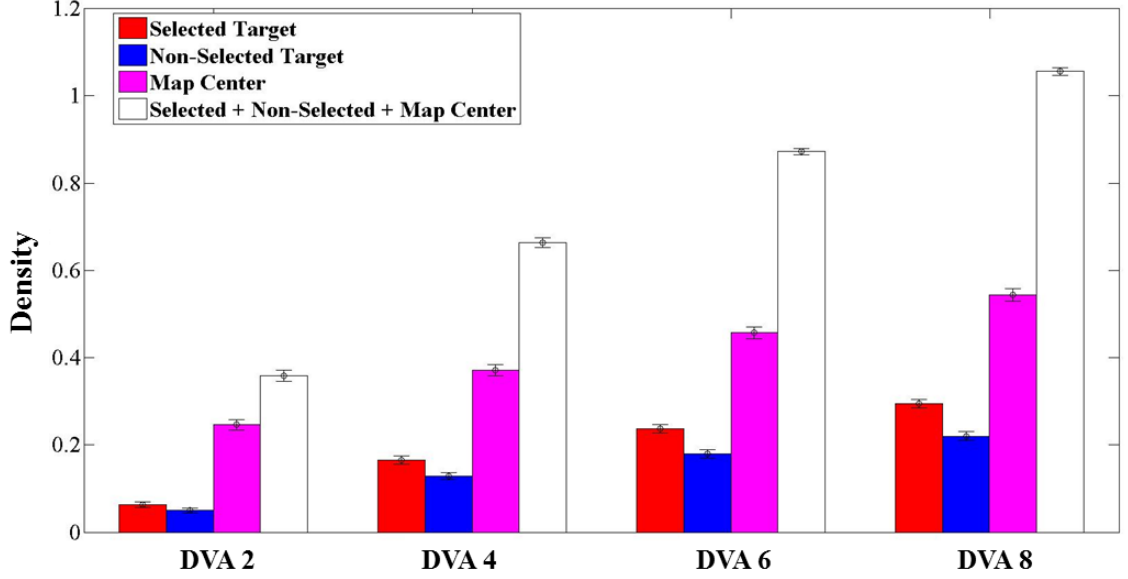


Figure 3.5: Average density (mean \pm SEM, $N = 236$ trials) of eye positions for selected targets (red), non-selected targets (blue), center of the map (magenta), and the combination of them (white), calculated in the circular areas of 2, 4, 6, and 8 degrees of visual angle radius centered on each one of them.

target and the center of the map, Fig. 3.5. We found that more than 50% of the mean density at 4 DVA, (0.664 ± 0.011 , mean \pm SEM), was attributed to both targets and the center of the stimulus (see white bars of Fig. 3.5). This means that most eye positions fell within a circular area of 4 DVA around these locations, suggesting that subjects were exploring and extracting spatial information to make a decision only within a small region around the targets and the center of the map. Since circular areas of 4 DVA centered on the targets and the center of the stimuli adequately captured most visual fixations during map exploration and did not overlap for all target configurations, for the following we will be considering circular regions of 4 DVA.

3.4.3 Time spending in exploring the alternative options and choice biases

We were also interested in investigating whether the choice of an option was related to the time that subjects spent exploring the area around it. Our initial hypothesis was that the time people spent looking at the selected targets was greater than the time they spent looking at the non-selected ones. To test this hypothesis, we considered only the eye positions that fell within the circular areas of 4 DVA radius around the targets, and calculated the mean relative density for the selected and non-selected targets across trials. Results revealed that subjects spent on average more time exploring the region around the selected location than the non-selected one, Fig.3.6. We also found that there was a significant association between the selected target and the target with the higher relative density ($\chi^2=4.207$, $P = 0.03$). These results are consistent with findings from a series of economic decision studies, which showed that the probability of choosing an item among many alternative options increases as a function of time that we look at it [35,36,80].

Moreover, there was a significant association between the selected target and the initially explored target, specifically, the circular area of 4 DVA radius centered on the initially explored target ($\chi^2 = 14.798$, $P = 1.196 \times 10^{-4}$). These results indicate that subjects had a strong bias to select the first option they explored. Also, they were more likely to choose the target that their last fixation was within the area of 4 DVA radius centered on that target ($\chi^2 = 78.059$, $P = 9.999 \times 10^{-19}$).

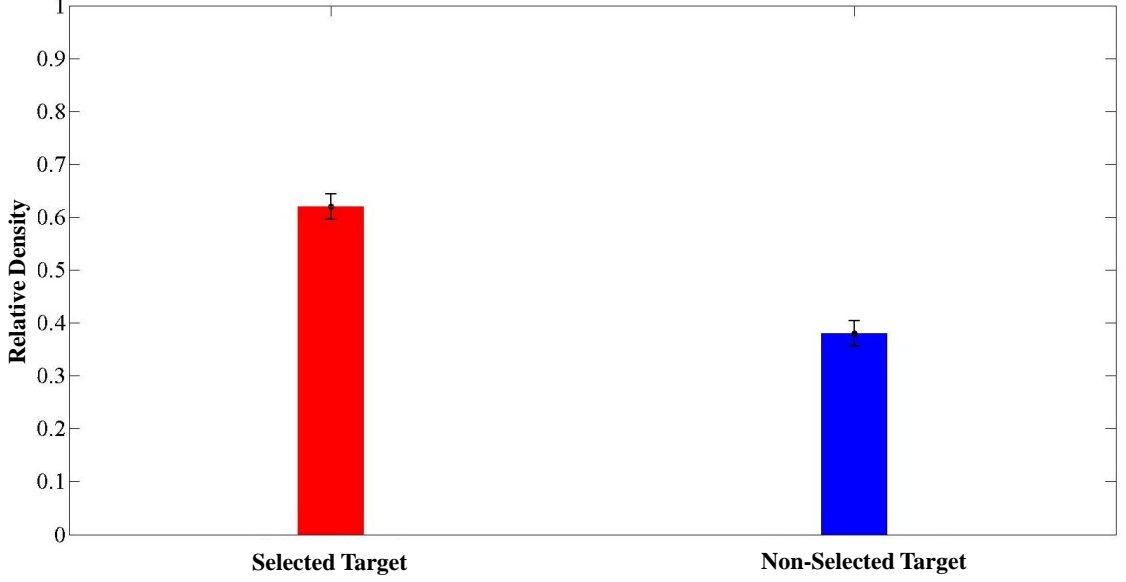


Figure 3.6: Average relative density of eye positions for selected and non-selected targets in the circular areas of 4 degrees of visual angle centered on each target (mean \pm SEM, $N = 209$ trials).

3.4.4 Comparison of alternative options as a function of time

We developed a novel approach to track the temporal evolution of map exploration in terms of the selected and non-selected targets. At every eye position $(eye_{x,t}, eye_{y,t})$ at time t , we computed the log-ratio of the Euclidean distance between the eye position and the selected target, to the Euclidean distance between the eye position and the non-selected target, Eq. 3.1. This measure provides a metric of how close is the current eye position to the selected target with respect to the non-selected one, with negative values corresponding to eye positions closer to the selected target, and vice-versa (see Materials and methods section for more details).

Characteristic examples of the log-ratio distance from different subjects and trials, and for different types of maps, are shown in Fig.3.7. Results indicate that subjects

were exploring the areas around the two alternative options, by repeatedly looking at them (i.e., log ratio distance values change from negative to positive, and vice-versa), irrespective of map type. Notice that similar “searching” behavior has been extensively documented in many value-based decision making studies, in which people were looking back and forth between options in order to compare their values and make a choice [35,36,80]. Hence, it is likely that subjects were continuously moving between the two alternative locations to compare them and select the best option.

By aligning the trials to the presentation of the stimulus, interestingly, we found that on average subjects showed a strong bias to move their eyes around the selected option from the very beginning, particularly 230 ms after stimulus onset, Fig.3.8. However, they did not make the decision at that time, but they evaluated the other option and compared the alternatives to select the best one.

To further explore the properties of the decision process, we aligned the trials to target selection onset, and computed the mean log-ratio of the Euclidean distances between the eye position and the selected target to the Euclidean distances between the eye position and the non-selected targets, for 1 s preceding choice selection, Fig.3.9. Interestingly, 345 ms before the selection of the target, subjects on average started moving their eyes close to the selected target (i.e., mean log ratio distance values became negative). Fig.3.10 illustrates the relation between the mean log-ratio distance and SEM for the 345 ms before the selection of the target. This relation was best described by a quadratic fit ($r^2=0.730$, $P=0.0001$), illustrating that the closer the eyes are getting to the selected target (i.e. negative values of the mean log ratio

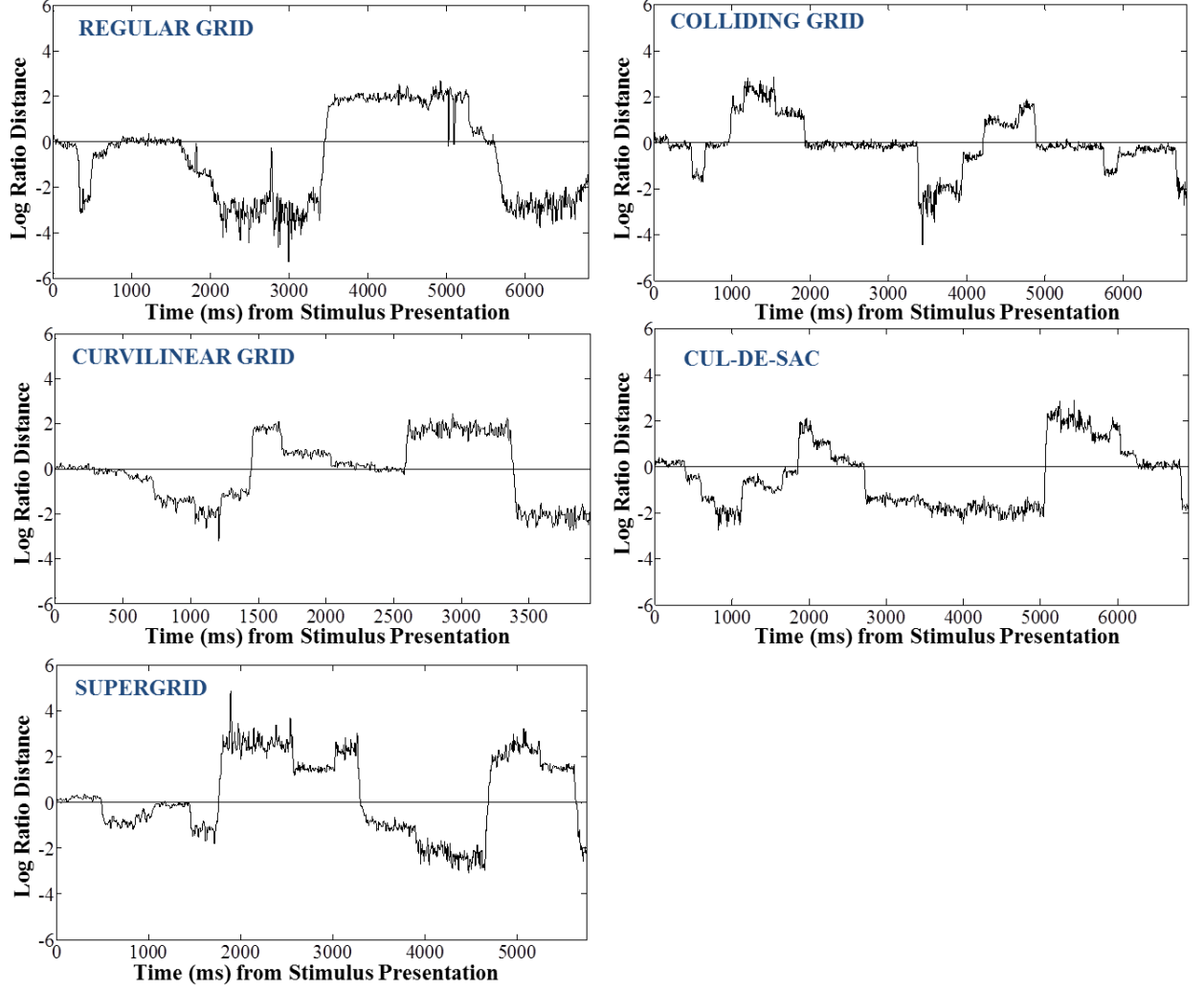


Figure 3.7: Example trials of single subjects while exploring different types of maps - one for each street network type - illustrating the *logarithmic ratio distance* (Eq. 3.1) of instantaneous eye positions to selected target over the non-selected target. Negative values of the log-ratio distance correspond to eye positions closer to the target ultimately selected, and vice-versa.

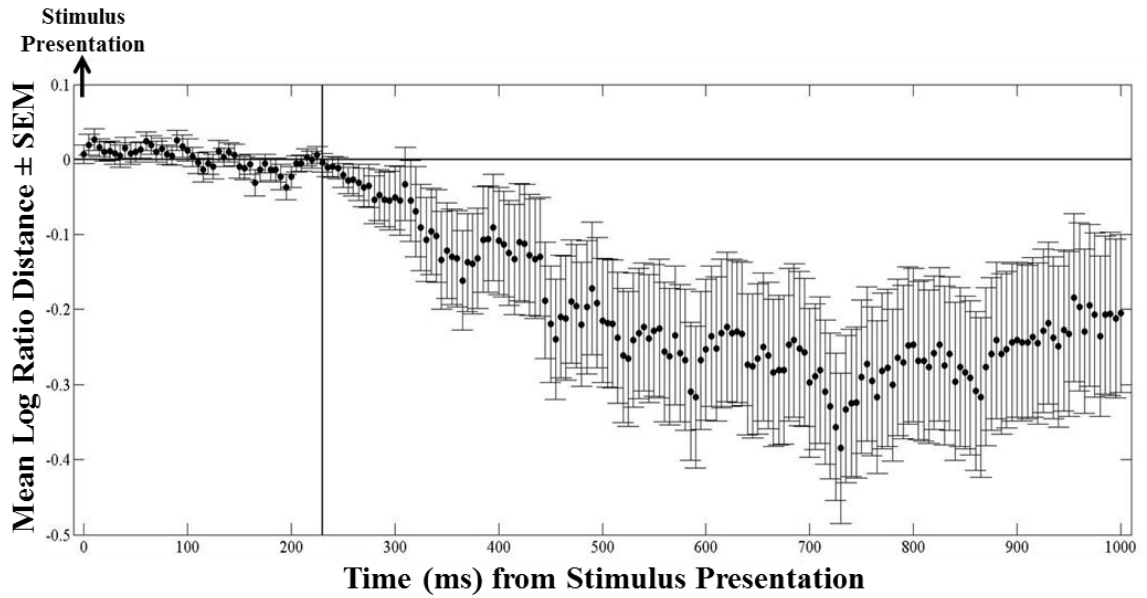


Figure 3.8: Mean logarithmic ratio (mean \pm SEM, $N = 236$ trials) of the Euclidean distance of the ongoing eye position to the selected target to the Euclidean distance of the eye position to the non-selected target, for 1 s after stimulus presentation. Trials are aligned to stimulus presentation. Notice that as early as 230 ms after stimulus onset, values of the mean log-ratio distance become negative (i.e., eyes are closer to the target ultimately selected).

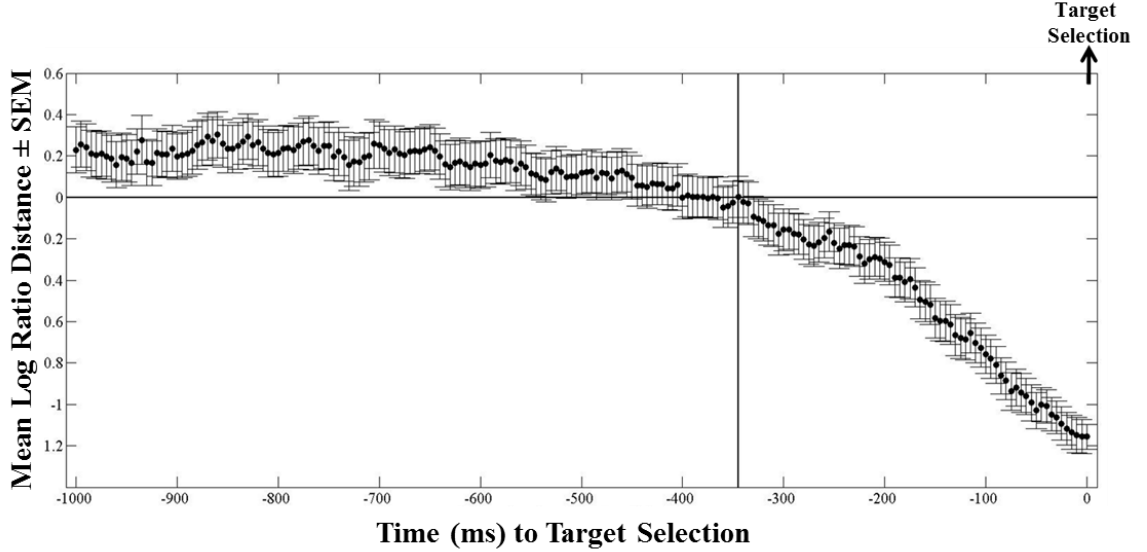


Figure 3.9: Mean logarithmic ratio (mean \pm SEM, $N = 236$ trials) of the Euclidean distance between the ongoing eye position and the selected target, to the distance between the eye position and the non-selected target, for 1 s before target selection. Trials are aligned to target selection. 345 ms before the selection of the target, mean log-ratio distance values become negative (i.e., subjects on average placed their eyes closer to the target ultimately selected).

distance), the lower the SEM becomes.

3.5 Discussion

The ability to explore novel environments and make spatial decisions, such as selecting a place to live or choosing a landmark to visit, is a fundamental and highly evolved behavior that requires the coordination of cognitive functions. In recent years, significant progress has been made in understanding the cognitive mechanisms of exploration and decision-making. Many studies have investigated how people and animals explore and navigate in novel environments [73, 74], whereas others have

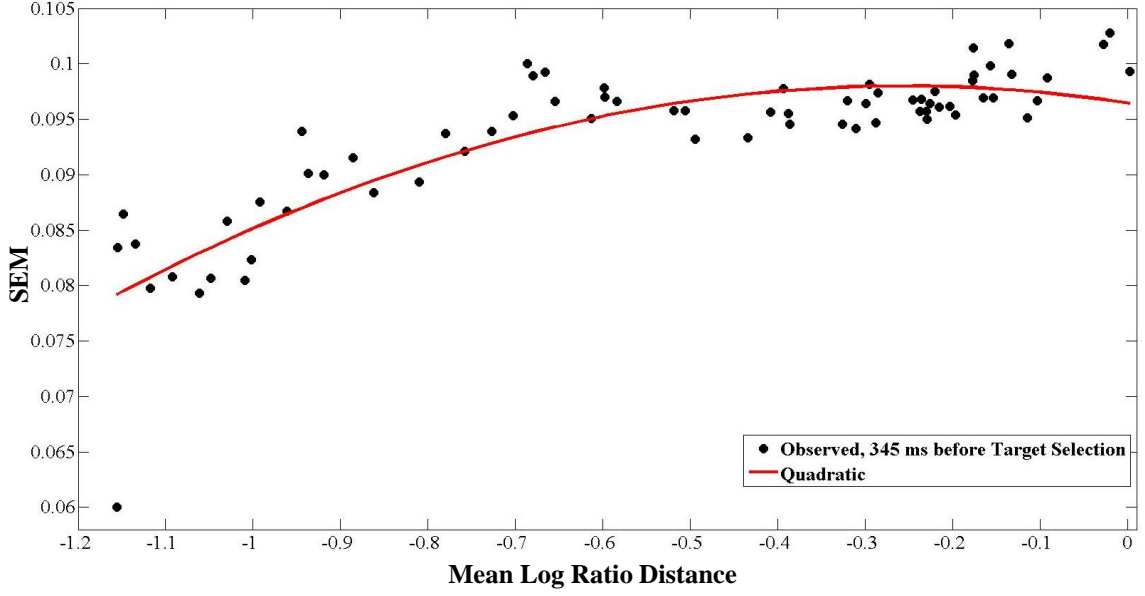


Figure 3.10: Mean Logarithmic Ratio Distance vs. SEM for the 345 ms before the selection of the target (see Fig.3.9). Red line describes the quadratic fit ($r^2=0.730$, $P=0.0001$) of this relation.

focused on understanding how they select between alternative options that have economic consequences [62, 80, 85]. Despite the important findings from these studies, little is known about the strategies that people and animals adopt when they are faced with both problems, i.e., exploring novel environments to make decisions. To address this question, we designed a psychophysical experiment to study how people make spatial decisions while exploring realistic environments. We used a variety of real maps of various U.S. cities with different street network layouts, and marked on each map two potential locations for a hypothetical Post Office. We recruited 12 subjects and asked them to choose one of the two alternative targets as the Post Office location, by moving a mouse cursor from the center of the map to the selected point.

Monitoring subjects' eye positions revealed that people developed highly stereo-

typed strategies for evaluating and comparing the two potential locations. Results showed that people followed a restricted exploration determined by the two targets and the center of the map. Particularly, subjects were continuously exploring the areas around the two targets before making a decision, by repeatedly looking back and forth between them. Although these findings are somehow in line with results from value-based decision studies [62,80], the interesting part is that people were not only fixating on the two potential locations, but they also spent a substantial amount of time looking at the center of the map. This finding was very consistent across all subjects and maps, irrespective of the map type and the configuration of the targets' locations. Even when the two targets were in close distance, and hence, eyes did not have to move through the center of the map, people spent time exploring the area around the map center. We have to point out that subjects had to place and hold the mouse cursor at the center of the screen before stimulus presentation, and move the cursor to the selected target upon deciding on their choice. Therefore, one could argue that exploration around the center of the map was due to the presence of the cursor, which triggered subjects' attention. However, this would have been a valid argument if the same effect had been observed in a similar study conducted in our lab, in which subjects were free to place a landmark at any possible location in realistic city maps [10]. The results of this study showed that people followed a wider exploration without spending much time looking at the maps' centers. Considering all these, we suggest that subjects explored the area around the centers of the maps to evaluate the two potential locations with respect to the centers. To be more specific,

holding the cursor at the center of the map, it is likely that subjects placed mentally themselves at the map center and computed the value of the alternative options with respect to their current location. This interpretation is consistent with spatial decisions we make in daily life, such as finding a place for dinner. The subjective value of an alternative option depends on many decision factors including also our current location. For instance, you may prefer a nearby restaurant rather than a better (in terms of quality of food) one which is located far away.

Another interesting finding was that eye fixations biased the decision towards the location that was being fixated most of time. This effect has been also described in value-based decision studies and is known as gaze-bias effect [35, 36, 59, 69–71, 80]. According to these studies, the longer you spend looking at a good you like, the higher the probability to select that good than the alternative options. For instance, before deciding which car to buy you may spend a lot of time test-driving and reviewing the car specifications. Recent computational theories developed to understand the gaze-bias effect, and suggest that when people are faced with multiple stimuli/items the brain assigns a relative decision variable to each of these alternatives and implements a comparison process by repeatedly looking at them [35, 36]. The relative decision variable assigned to an item is positively correlated with the time that subjects fixate on it [35, 36, 80]. Hence, the probability to select an item increases the longer the item is fixated on. According to these findings, we may also assume that when subjects are spending more time exploring the area around one of the alternative locations, the value of this location increases, and hence, it is likely to select this target as the

Post Office location.

One of the key findings in the current study is that the target that was initially being fixated was significantly correlated with the final choice. In other words, people showed a strong bias to select the location that they firstly explored after the trial onset. This bias appeared at around 230 ms after the presentation of the stimulus. Similar findings have also been reported in many studies involving choices between multiple goods which showed that the probability of first-seen item is chosen increases with the duration of the first fixation [35]. Additionally, a recent study explored the neural basis of choice bias using magnetoencephalography in a value-based decision task and found that MEG signal deviations from biased decisions occurred as early as 250-750 ms following the stimulus onset [26].

Finally, we found that subjects were more likely to choose the target that their last fixation was at. Subjects shifted the fixation around the selected location at about 345 ms prior to make a decision. All these findings suggest that humans adopted highly stereotyped strategies to explore novel environments and make spatial decisions. These strategies share many common characteristics with the strategies that people follow to make decisions between options that have economic consequences.

Chapter 4

Concluding Remarks

4.1 Summary

It is generally believed that the brain of different species, including humans, has evolved in a way that individuals are capable of exploring and navigating efficiently within the environment. It is almost certain that none of the species would be able to survive in hostile environments if they were not able to efficiently search for food, avoid predators, and find places to live. Despite many years of research, it is still poorly understood how people and animals explore the external world to generate internal cognitive maps that can be retrieved to make decisions and select actions (e.g., choose a restaurant to have dinner tonight, avoid busy main roads during traffic jam, etc.). For many years, scientists aimed to address this question by focusing in neurophysiological studies in animals or functional imaging in humans using mainly simple experimental set-ups. Even though these studies greatly contributed in reveal-

ing some of the mechanisms underlying exploration and navigation, little is known on what information people extract about spatial characteristics of the environment, and how this information is coded into the brain to make spatial decisions.

The primary goal of this thesis is to understand the behavioral and neural mechanisms underlying processing of spatial information, acquired during exploration of realistic environments to make spatial decisions. We designed a novel task, in which subjects had to explore maps from various U.S. cities to decide where to build a City Hall, while neuromagnetic fluxes were recorded from their heads using a whole-head MEG device. We found that ongoing neuronal activity in a network of cortical regions was associated with particular spatial parameters of the city maps. This network involved predominantly the right frontal and prefrontal areas of the brain, suggesting that these areas have an important role in processing spatial information for making decisions. Additionally, we found other brain areas also involved in the processing of spatial information, such as right temporal areas and cerebellum. These results indicate that processing spatial information for making a decision is a complex process that requires the involvement of more than one regions. Finally, we found that the associations between ongoing neural activity and spatial parameters were modulated by the type of the map. This suggests that, depending on the type of the map, people may use different spatial information to explore the map and make a spatial decision.

We also studied how people make spatial decisions in realistic environments when they were forced to select between a limited menu of choices. In this experiment, individuals had to explore maps from various U.S. cities, and to select between two

locations to build a hypothetical Post Office. We recorded subjects' eye positions and analyzed the gaze behavior to characterize how people explore maps to select between these options. We found that subjects adopted a highly stereotypical gaze behavior to evaluate the alternative options. In particular, they were continuously exploring the areas around the two options and the center of the map, by looking back and forth between them before making a decision. Unlike economic choices, in which people follow similar strategies by looking repeatedly at the available options, in our experiment individuals were also exploring the area around the center of the map. These findings suggest that subjects might place themselves at the center of the map and evaluated the alternative options with respect to their current location. We also found other similarities with economic choice paradigms, such as people spent more time exploring the area around the selected option than the non-selected one. Finally, subjects showed a strong bias to select the option they firstly explored. We interpret all these findings as evidence that the “attractiveness” of a location is biased by the time spending to explore that location, and the initial fixations around an option favor the location ultimately chosen.

4.2 Broader impacts

The findings presented in this thesis suggest new avenues to elucidate the behavioral and neural mechanisms underlying exploration and spatial decision-making. These findings are important from the standpoint of both engineering innovation and the

organization of the brain. For instance, civil engineers could adopt our approach to identify important spatial features acquired during exploration of realistic environments to make spatial decisions. In that way, they could identify more “attractive” locations to build landmarks, shopping malls, and apartment buildings.

Such findings can also inspire further studies in understanding the functional role of brain regions involved in spatial information processing. For instance, using animal models (e.g., rodents, monkeys) we are able to perturb brain regions via either microstimulation or reversible pharmacological inactivation, and observe the effects on the exploration and decision making. For instance, it would be interesting to see how the inactivation of regions involved in processing of spatial parameters affects the ability to efficiently explore the external world and make spatial decisions.

Finally, the proposed methodology on the MEG study could be used to understand the pathophysiology of neurological disorders that lead to deficits in processing spatial information and decision-making. For instance, “right hemisphere damage” (RHD) patients frequently have difficulty in following directions or exploring and navigating around buildings. Although the pathophysiology of this disorder is not clear yet, neurologists have associated it with deficits in processing spatial information. It would be interesting to run the MEG study presented in this thesis on RHD patients and explore potential changes in the processing of spatial parameters from maps.

Bibliography

- [1] N. Aggelopoulos and E. Rolls. Scene perception: inferior temporal cortex neurons encode the positions of different objects in the scene. *Eur J Neurosci.*, 22:2903–2916, 2005.
- [2] G. Aguirre, J. Detre, D. Alsop, and M. D’Esposito. The parahippocampus subserves topographical learning in man. *Cerebral cortex (New York, N.Y. : 1991)*, 6(6):823–829, 1996.
- [3] M. Basso and R. Wurtz. Modulation of neuronal activity in superior colliculus by changes in target probability. *J Neurosci.*, 18(18):7519–34, 1998.
- [4] M. Blades and L. Medlicott. Developmental differences in the ability to give route directions from a map. *J. Environ. Psychol.*, 12:175–185, 1992.
- [5] G. Box, G. Jenkins, and G. Reinsel. *Time series analysis: forecasting and control*. GoldenDay, 2008.
- [6] L. Brown. *The story of maps*. New York: Dover, 1949.
- [7] D. Bryant and B. Tversky. Mental representations of spatial relations from diagrams and models. *Journal of Experimental Psychology: Learning, Memory and Cognition.*, 25:137–156, 1999.
- [8] N. Burgess, S. Becker, J. King, and J. O’Keefe. Memory for events and their spatial context: models and experiments. *Philosophical transactions of the Royal Society of London. Series B, Biological sciences*, 356(1413):1493–1503, 2001.
- [9] M. Chafee, B. Averbeck, D. Crowe, and G. AP. Impact of path parameters on maze solution time. *Arch Ital Biol.*, 140:247251, 2002.
- [10] P. Christova, M. Scoppa, J. Peponis, and A. Georgopoulos. Exploring small city maps. *Exp. Brain Res.*, 223(2):207–217, 2012.
- [11] P. Cisek. Cortical mechanisms of action selection: The affordance competition hypothesis. *Philos Trans R Soc Lond B Biol Sci.*, 362(1485):1585–99, 2007.

- [12] P. Cisek and J. Kalaska. Simultaneous encoding of multiple potential reach directions in dorsal premotor cortex. *J Neurophysiol.*, 87(2):1149–54, 2002.
- [13] P. Clark and F. Evans. Distance to nearest neighbor as a measure of spatial relationships in populations. *Ecology*, 35:445–453, 1954.
- [14] B. Coe, K. Tomihara, M. Matsuzawa, and O. Hikosaka. Visual and anticipatory bias in three cortical eye fields of the monkey during an adaptive decision-making task. *J Neurosci.*, 22:5081–5090, 2002.
- [15] R. Conroy Dalton. The secret is to follow your nose. *Environ Behav*, 35:107131, 2003.
- [16] P. Corlett, M. Aitken, A. Dickinson, D. Shanks, G. Honey, R. Honey, T. Robbins, E. Bullmore, and P. Fletcher. Prediction error during retrospective revaluation of causal associations in humans:fmri evidence in favor of an associative model of learning. *Neuron*, 44:877–888, 2004.
- [17] D. Crowe, B. Averbeck, M. Chafee, J. Anderson, and A. Georgopoulos. Mental maze solving. *J Cogn Neurosci.*, 12:813–827, 2000.
- [18] H. Cui and R. Andersen. Posterior parietal cortex encodes autonomously selected motor plans. *Neuron*, 56:552–559, 2007.
- [19] A. Damasio. *Descartes’ Error: Emotion, Reason, and the Human Brain*. Putnam Adult, 1994.
- [20] D. de Araujo, O. Baffa, and R. Wakai. Theta oscillations and human navigation: A magnetoencephalography study. *Journal of Cognitive Neuroscience*, 14:70–78, 2002.
- [21] M. Dorris and P. Glimcher. Activity in posterior parietal cortex is correlated with the relative subjective desirability of action. *Neuron.*, 44:365–378, 2004.
- [22] A. D. Ekstrom, M. J. Kahana, J. B. Caplan, T. A. Fields, E. A. Isham, E. L. Newman, and I. Fried. Cellular networks underlying human spatial navigation. *Nature*, 425(6954):184–188, 2003.
- [23] C. Feierstein, M. Quirk, N. Uchida, D. Sosulski, and Z. Mainen. Representation of spatial goals in rat orbitofrontal cortex. *Neuron*, 51:495–507, 2006.
- [24] M. Glaholts and E. Reingold. The time course of gaze bias in visual decision tasks. *Visual Cognition*, 7(18):1228–1243, 2009.
- [25] T. Hafting, M. Fyhn, S. Molden, M.-B. Moser, and E. I. Moser. Microstructure of a spatial map in the entorhinal cortex. *Nature*, 436(7052):801–806, 2005.

- [26] W. Hedgecock, D. Crowe, A. Leuthold, and A. Georgopoulos. A magnetoencephalography study of choice bias. *Exp. Brain Res.*, 202(1):121–127, 2010.
- [27] B. Hillier. *Space is the Machine*. Cambridge: Cambridge University Press, 1996.
- [28] B. Hillier, R. Burdett, J. Peponis, and A. Penn. Creating life: or does architecture determine anything? *Arch Comport Arch Behav*, 3:233–250, 1987.
- [29] B. Hillier and S. Iida. *COSIT 2005*, chapter Network and psychological effects of urban movement. Springer, 2005.
- [30] B. Hillier, A. Penn, J. Hanson, T. Grajewski, and J. Xu. Natural movement: or configuration and attraction in urban pedestrian movement. *Environ Plan B*, 20:29–66, 1993.
- [31] S. HJ, N. Burgess, E. Maguire, S. Baxendale, T. Hartley, P. Thompson, and J. O’Keefe. Unilateral temporal lobectomy patients show lateralized topographical and episodic memory deficits in a virtual town. *Brain*, 124:2476–2489, 2001.
- [32] G. Janzen and M. van Turenout. Selective neural representation of objects relevant for navigation. *Nature Neuroscience*, 7:673–677, 2004.
- [33] G. Jenkins and D. Watts. *TSpectral Analysis and Its Application*. GoldenDay, 1968.
- [34] M. Kahana, R. Sekuler, J. Caplan, M. Kirschen, and J. Madsen. Human theta oscillations exhibit task dependence during virtual maze navigation. *Nature*, 399:781–784, 1999.
- [35] I. Krajbich, C. Armel, and A. Rangel. Visual xations and the computation and comparison of value in simple choice. *Nat Neurosci.*, 13:12921298, 2010.
- [36] I. Krajbich and A. Rangel. Multialternative drift-diffusion model predicts the relationship between visual xations and choice in value-based decisions. *Proc Natl Acad Sci USA*, 108:1385213857, 2010.
- [37] F. Langheim, A. Leuthold, and A. Georgopoulos. Synchronous dynamic brain networks revealed by magnetoencephalography. *Proc Natl Acad Sci USA*, 2005.
- [38] A. Leuthold. Subtraction of heart artifact from meg data: the matched filter revisited. Soc Neurosci Abstracts, 2003.
- [39] A. Leuthold, F. Langheim, S. Lewis, and A. Georgopoulos. Time series analysis of magnetoencephalographic data during copying. *Exp Brain Res*, 2005.
- [40] E. Maguire, N. Burgess, J. Donnett, R. Frackowiak, F. CD, and O. J. Knowing where and getting there: A human navigation network. *Science*, 280:921–924, 1998.

- [41] E. Maguire, T. Burke, J. Phillips, and H. Staunton. Topographical disorientation following unilateral temporal lobe lesions in humans. *Neuropsychologia*, 34(10):993–1001, 1996.
- [42] E. Maguire, R. Frackowiak, and C. Frith. Recalling routes around london: activation of the right hippocampus in taxi drivers. *J Neuroscience*, 17:7103–7110, 1998.
- [43] R. McPeck and E. Keller. Deficits in saccade target selection after inactivation of superior colliculus. *Nat Neurosci.*, 7:757763, 2004.
- [44] J. O’Doherty. Contribution of the ventromedial prefrontal cortex to goal-directed action selection. *Ann N Y Acad Sci.*, 1239:118–129, 2011.
- [45] J. O’Keefe and J. Dostrovsky. The hippocampus as a spatial map. preliminary evidence from unit activity in the freely-moving rat. *Brain Research*, 34:171–175, 1971.
- [46] J. O’Keefe and L. Nadel. *The Hippocampus as a Cognitive Map*. Oxford University Press, 1978.
- [47] J. O’Keefe and M. Recce. Phase relationship between hippocampal place units and the eeg theta rhythm. *Hippocampus*, 3:317330, 1993.
- [48] C. Padoa-Schioppa. Orbitofrontal cortex and the computation of economic value. *Ann N Y Acad Sci.*, 1121:232–253, 2007.
- [49] C. Padoa-Schioppa. Neurobiology of economic choice: a good-based model. *Annu Rev Neurosci.*, 34:333–359, 2011.
- [50] C. Padoa-Schioppa. Neurobiology of economic choice: a good-based model. *Annu Rev Neurosci.*, 34:333–359, 2011.
- [51] C. Padoa-Schioppa and J. Assad. Neurons in orbitofrontal cortex encode economic value. *Nature*, 44:223–226, 2006.
- [52] C. Padoa-Schioppa and X. Cai. The orbitofrontal cortex and the computation of subjective value: consolidated concepts and new perspectives. *Ann N Y Acad Sci.*, 1239:130–137, 2011.
- [53] A. Pastor-Bernier and P. Cisek. Neural correlates of biased competition in premotor cortex. *J Neurosci.*, 31(19):7083–7088, 2011.
- [54] A. Penn, B. Hillier, D. Banister, and X. J. Configurational modeling of urban movement networks. *Environ Plan B*, 25:5984, 2008.
- [55] J. Peponis, S. Bafna, and Z. Zhang. The connectivity of streets: reach and directional distance. *Environ Plan B*, 35:881–901, 2008.

- [56] J. Peponis, E. Hadjinikolaou, C. Livieratos, and D. Fatouros. The spatial core of urban culture. *Ekistic*, 334(335):43–55, 1989.
- [57] J. Peponis, C. Ross, and M. Rashid. The structure of urban space, movement and co-presence: the case of atlanta. *Geoforum*, 28:341358, 1997.
- [58] J. Peponis and J. Wineman. *Handbook of Environmental Psychology*, chapter The Spatial Structure of Environment and Behavior. New York: John Wiley and Sons, 2002.
- [59] R. Pieters and L. Warlop. Visual attention during brand choice: the impact of time pressure and task motivation. *International Journal of Research in Marketing*, 16:1–16, 1999.
- [60] M. Platt and P. Glimcher. Neural correlates of decision variables in parietal cortex. *Nature.*, 400:233–238, 1999.
- [61] V. Prevosto, W. Graf, and G. Ugolini. Cerebellar inputs to intraparietal cortex areas lip and mip: functional frameworks for adaptive control of eye movements, reaching, and arm/eye/head movement coordination. *Cereb. Cortex*, 20:214228, 2010.
- [62] A. Rangel and J. Clithero. *The computation of stimulus values in simple choice. Neuroeconomics*. Elsevier Inc., 2007.
- [63] K. Ridderinkhof, M. Ullsperger, E. Crone, and S. Nieuwenhuiss. The role of the medial frontal cortex in cognitive control. *Science*, 306:443–447, 2004.
- [64] R. Robertson, E. Rolls, and P. Georges-Francois. Spatial view cells in the primate hippocampus: effects of removal of view details. *J. of Neurophysiol.*, 79(3):1145–1156, 1998.
- [65] C. Rochefort, J. Lefort, and L. Rondi-Reig. The cerebellum: a new key structure in the navigation system. *Front. Neural Circuits*, 7:1–12, 2013.
- [66] M. Roesch and C. Olson. Neuronal activity related to reward value and motivation in primate frontal cortex. *Science*, 304:307–310, 2004.
- [67] E. Schottera, R. Berrya, C. McKenziea, and K. Raynera. Gaze bias: Selective encoding and liking effects. *Visual Cognition*, 18(8):1113–1130, 2010.
- [68] W. Scoville and B. Milner. Loss of recent memory after bilateral hippocampal lesions. *J Neurol Neurosurg Psychiatry*, 20:11–21, 1957.
- [69] S. Shimojo, C. Simion, E. Shimojo, and C. Scheier. Gaze bias both reflects and influences preference. *Nat Neurosci.*, 6:13171322, 2003.

- [70] C. Simion and S. Shimojo. Early interactions between orienting, visual sampling and decision making in facial preference. *Vision Res.*, 46:3331–3335, 2006.
- [71] C. Simion and S. Shimojo. Interrupting the cascade: orienting contributes to decision making even in the absence of visual stimulation. *Percept Psychophys.*, 69:591595, 2007.
- [72] L. Snyder, K. Grieve, P. Brothie, and R. Andersen. Separate body- and world-referenced representations of visual space in parietal cortex. *Nature*, 394(6696):887–891, 1998.
- [73] H. Spiers and E. Maguire. Thoughts, behaviour, and brain dynamics during navigation in the real world. *Neuroimage*, 31:1826–1840, 2006.
- [74] H. Spiers and E. Maguire. A navigational guidance system in the human brain. *Hippocampus*, 17:618–626, 2007.
- [75] L. Sugrue, G. Corrado, and W. Newsome. Choosing the greater of two goods: Neural currencies for valuation and decision making. *Nat Rev Neurosci.*, 6:363–375, 2005.
- [76] W. Suzuki and D. Amaral. Perirhinal and parahippocampal cortices of the macaque monkey: Cortical afferents. *Journal of Comparative Neurology*, 350:497–533, 1994.
- [77] J. Taube, R. Muller, and J. Ranck. Head-direction cells recorded from the post-subiculum in freely moving rats. 1. description and quantitative analysis. *J Neurosci.*, 10:420–435, 1990.
- [78] H. Taylor and B. Tversky. Perspective in spatial descriptions. *Journal of Memory and Language*, 35:371–391, 1996.
- [79] E. Tolman. Cognitive maps in rats and men. *Psychological Review*, 55:189–208, 1948.
- [80] R. Towal, M. Mormann, and C. Koch. Simultaneous modeling of visual saliency and value computation improves predictions of economic choice. *Proc Natl Acad Sci USA.*, 110:3858–3867, 2013.
- [81] G. Veneri, A. Federico, and A. Rufa. Evaluating the influence of motor control on selective attention through a stochastic model: the paradigm of motor control dysfunction in cerebellar patient. *Biomed Res Int.*, 2014:1–13, 2014.
- [82] J. Wallis. Orbitofrontal cortex and its contribution to decision-making. *Annu. Rev. Neurosci.*, 30:31–56, 2007.

- [83] J. Wiener, C. Holscher, S. Buchner, and L. Konieczny. Gaze behaviour during space perception and spatial decision making. *Psychol Res.*, 76:713–729, 2012.
- [84] M. Wilke, I. Kagan, and R. Andersen. Functional imaging reveals rapid reorganization of cortical activity after parietal inactivation in monkeys. *Proc Natl Acad Sci U S A.*, 109(21):8274–8279, 2012.
- [85] K. Wunderlich, A. Rangel, and J. O’Doherty. Economic choices can be made using only stimulus values. *Proc Natl Acad Sci USA.*, 107(34):15005–15010, 2010.